UNIVERSITY OF SOUTHAMPTON

Disc Winds Matter: Modelling Accretion and Outflow on All Scales

by

James Matthews

A thesis submitted in partial fulfillment for the degree of Doctor of Philosophy

in the
Faculty of Physical Sciences and Engineering
Department of Physics & Astronomy

March 2016

UNIVERSITY OF SOUTHAMPTON

Abstract

Faculty of Physical Sciences and Engineering
Department of Physics & Astronomy

Doctor of Philosophy

by James Matthews

The Thesis Abstract is written here (and usually kept to just this page). The page is kept centered vertically so can expand into the blank space above the title too...

Contents

Abstract **i**

1 Introduction **1**
1.1 The Physics of Accretion . . . 3
1.1.1 Spherical Accretion and The Eddington Limit . . . 4
1.1.2 Accretion Discs . . . 5
1.1.2.1 Steady-state Accretion Discs: The α-prescription . . . 5
1.2 Accreting Compact Binaries . . . 8
1.2.1 Roche Lobe-Overflow . . . 10
1.2.2 Cataclysmic Variables . . . 11
1.2.2.1 Dwarf Novae and the Disc-instability Model . . . 11
1.2.2.2 Nova-like Variables . . . 12
1.2.3 Low Mass X-ray Binaries . . . 14
1.3 Quasars and Active Galactic Nuclei . . . 14
1.3.1 AGN Unification and the dusty Torus . . . 16
1.3.2 X-ray Properties of AGN . . . 19
1.3.2.1 The Soft X-ray Excess . . . 20
1.3.3 The Broad Line Region and Connection to Outflows . . . 21
1.4 The Current Understanding of the Disc Continuum . . . 21
1.4.1 The Spectral shape of CV discs . . . 22
1.4.2 The Big Blue Bump in AGN . . . 23
1.4.2.1 Fitting AGN Spectra . . . 23
1.4.2.2 The 1000Å Break . . . 23
1.4.2.3 The Accretion Disc Size Problem . . . 23
1.5 The Universality of Accretion . . . 24
1.5.1 The RMS-flux relation . . . 24
1.5.2 Accretion States . . . 25
1.5.3 Jets and Outflows . . . 25
1.5.4 A Global Picture . . . 25

2 Accretion Disc Winds **26**
2.1 Observational Evidence . . . 26
2.1.1 Cataclysmic Variables . . . 27
2.1.2 X-ray Binaries . . . 29
2.1.3 AGN and Quasars . . . 30
2.1.3.1 Broad Absorption Line Quasars . . . 30

2.1.3.2 Warm Absorbers 30
2.1.3.3 Ultra-fast Outflows 30
2.1.4 Stellar Winds 30
2.1.4.1 Clumping 31
2.2 Driving Mechanisms 31
2.2.1 Thermal Winds 32
2.2.2 Radiatively Driven Winds 33
2.2.3 Line-driven Winds 33
2.2.4 Magneto-centrifugal Winds 33
2.3 Accretion Disc Wind Models 33
2.4 A Kinematic Prescription 33
2.5 The really, really big picture: AGN Feedback 33
2.5.1 Observational evidence for feedback 33
2.5.2 Radiative or quasar mode feedback 35
2.5.3 Kinetic or radio mode feedback 35
2.5.4 In-situ Explanations 35

Bibliography **36**

Chapter 1

Introduction

"And now you're asking, I don't know where to begin"
Mike Vennart, Silent/Transparent

The release of gravitational potential energy as mass falls towards a compact object is the most efficient energetic process in the universe, even more efficient than nuclear fusion. This *accretion* process is thought to power the huge radiative engines at the centres of every galaxy – accreting supermassive black holes known as active galactic nuclei (AGN). As the matter falls into the potential well of the black hole it often forms an accretion disc, which, in many cases, is an efficient radiator of the gravitational energy released. In some cases, the accretion disc can outshine the entire stellar population of the galaxy, appearing as a quasi-stellar object (QSOS) or *quasar*. As well as powering, AGN, accretion discs are present in X-ray binaries (XRBs), young-stellar objects (YSOs) and cataclysmic variables (CVs). Accretion is a universal process; broadly speaking, the physics is similar of whether matter is falling on to a $\sim 1\ M_{\odot}$ Neutron Star or White Dwarf system, or a $\sim 10^{10}\ M_{\odot}$ black hole.

Outflows are ubiquitous in accreting systems. We see collimated radio jets in AGN (Hazard et al. 1963; Potash and Wardle 1980; Perley et al. 1984; Marscher 2006) and XRBs (Belloni 2010), and there is even evidence of extended radio emission in CVs (Benz et al. 1983; Coppejans et al. 2015). These radio jets tend to appear in specific accretion states (Fender 2001; Fender et al. 2004; Körding et al. 2008), implying an intrinsic connection to the accretion process. Even more intriguing, in XRBs less collimated, mass-loaded outflows or *winds* are observed in the opposite accretion state, possibly emanating from the accretion disc. Evidence for disc winds is widespread across the mass range, but perhaps the most spectacular indication is the blue-shifted, broad absorption lines (BALs) in the rest-frame ultraviolet (UV) seen in high-state CVs (Heap et al. 1978; Greenstein and Oke 1982; Cordova and Mason 1982) and the so-called broad absorption line quasars (BALQSOs) that make up 20−40% of quasars (Weymann et al. 1991; Knigge et al. 2008; Allen et al. 2011). BALs and 'P-Cygni' profiles (Struve 1935; Rottenberg 1952) are also seen in stellar winds (e.g. Cassinelli 1979) and sometimes even in the optical spectra of CVs (Patterson et al. 1996; Ringwald and Naylor 1998; Kafka and Honeycutt 2004). Broad, blue-shifted absorption is even observed in the Fe Kα line in AGN (Reeves et al. 2003; Pounds and Reeves 2009; Tombesi et al. 2010) – these are known as ultra-fast outflows or UFOs[1].

The astrophysical significance of disc winds extends, quite literally, far beyond the accretion environment. They offer a potential mechanism by which the central accretion engine can interact with the host galaxy and interstellar medium via a 'feedback' mechanism (King 2003; Fabian 2012). Feedback is required in models of galaxy evolution (Springel et al. 2005) and may explain the famous '$M - \sigma$' relation (Silk and Rees 1998; Häring and Rix 2004). Winds also offer a natural way to *unify* much of the diverse phenomenology of AGN, CVs and XRBs. The principle of unification can be applied along more than one 'axis' of parameter space. For example, there exist elegant models that attempt to explain *all* of the behaviour of quasars with only a central black hole, a jet, an accretion disc, and an associated outflow, by varying the viewing angle (Elvis 2000). Similarly elegantly, it has been shown that much of the behaviour of XRBs is directly applicable to AGN (McHardy et al. 2006), and models of outflows in CVs have been successfully 'scaled-up' and applied to quasars and AGN (e.g. Higginbottom et al. 2013).

Despite their clear importance and ubiquity, there are still many unanswered questions relating to the true impact of winds and their underlying physical origins. Here, I aim to address some of these questions, and take steps towards building a more holistic picture of the impact of winds on the spectral appearance and accretion physics of disc systems. This thesis is structured as follows. In the remainder of this chapter, I will

[1]It should be noted that, while X-ray spectral fitting can be somewhat of a dark art, the explanations for these UFOs are somewhat more believable than their sci-fi namesakes.

give the background accretion theory and detail the successes and failures of accretion disc models when compared to observations, as well as describing the different classes of accreting objects in more detail. In chapter 2, I dedicate some time to specifically discussing the theory of, and observational evidence for, accretion disc winds. In chapter 3, I outline the Monte Carlo radiative transfer (MCRT) and photoionization methods I have used in order to investigate the impact of disc winds on the spectra of accreting systems. The science chapters contain three separate submitted papers, in which we investigated the impact of disc winds on the spectra of CVs (Chapter 5), and tested disc wind quasar unification models (Chapters 6 and 7). In chapter 8, I summarise my findings and their astrophysical significance, and discuss potential avenues for future work.

1.1 The Physics of Accretion

The basic phenomenon of accretion- matter falling into a gravitational potential well- is a ubiquitous one in astrophysics. The energy, ΔE, released by a parcel of mass Δm falling from infinity onto an object of mass M and radius R_* is given by

$$\Delta E = \frac{GM\Delta m}{R_*}, \tag{1.1}$$

meaning that the accretion power can then be given by

$$L_{acc} = \frac{GM\dot{M}}{R}. \tag{1.2}$$

We can also parameterise any energetic process with the form

$$\Delta E = \eta \dot{M} c^2, \tag{1.3}$$

where η is some efficiency. Nuclear fusion is one of the more efficient energetic processes in the universe, with an efficiency of $\eta = 0.007$. If we rearrange the above equations in terms of η we find

$$\eta = \frac{G}{c^2}\frac{M}{R}. \tag{1.4}$$

In other words, the efficiency of accretion is directly related to the *compactness* of the central object. Values of compactness for four different compact objects are shown in table **??**.

1.1.1 Spherical Accretion and The Eddington Limit

The simplest geometry one might propose for accretion would be one in which a central mass accretes matter from an all-encompassing cloud or the inter-stellar medium. The process of spherical accretion has come to be known as Bondi-Hoyle-Lyttleton accretion (Hoyle and Lyttleton 1939; Bondi and Hoyle 1944). In particular, Bondi (1952) studied spherically symmetric accretion onto a point mass and derived the Bondi radius,

$$r_B = \frac{GM}{c_S^2}, \tag{1.5}$$

where $c_S = c_S(r_B)$ is the sound speed as a function of radius. The Bondi radius represents a critical point inside which the material is supersonic and will accrete on the free-fall timescale.

When this timescale is long enough, then the accreting matter can radiate its potential energy with luminosity L. This radiation will induce a force on electrons, given by

$$F_{rad} = \frac{L\sigma_T}{4\pi r^2 c}, \tag{1.6}$$

where $\sigma_T = 6.65 \times 10^{-25}\mathrm{cm}^2$ is the Thomson cross-section. If this radiation force term dominates over the gravitational force then the material will no longer fall inwards. Consider radiation pressure acting on electron-proton pairs, for which the gravitational force is approximately given by GMm_p/r^2. Combining this expression with equation 1.6 gives a natural maximum accretion luminosity, known as the *Eddington limit*, of

$$L_{Edd} = \frac{4\pi GMm_pc}{\sigma_T}, \tag{1.7}$$

with an associated Eddington accretion rate of

$$\dot{M}_{Edd} = \frac{L_{Edd}}{\eta c^2}. \tag{1.8}$$

The Eddington limit makes a number of assumptions, namely that the accretion flow is steady, spherically symmetric, ionized, and has its opacities dominated by electron scattering. Clearly, there are many astrophysical situations where this does not hold. For example, the recent outburst of V404 Cyg showed wildly variable luminosities on short timescales (see, e.g., Kuulkers et al. 2015; Motta et al. 2015, among many, many ATels), and in any binary system or disc dominated system then the assumption of spherical symmetry will break down. Nevertheless, the Eddington limit gives a good order of magnitude estimate of the maximum luminosity of an accreting object, and also provides a useful way of parameterising accretion rate, as it scales linearly with mass. It can also be used to characterise the *state* of an accretion disc. In general, sources around 0.1 L_{Edd} find themselves in a soft or thin-disc state (REFs), whereas for much lower Eddington fractions sources will be dominated by advection and form radiatively-ineffient accretion flows (RIAFs; REFs). It is also clear that around the Eddington limit radiation pressure must play a major role in determining the disc morphology (see section 2.2.2).

1.1.2 Accretion Discs

In many astrophysical situations – for example, binary orbits and gas clouds orbiting BHs – any accreting matter will possess some net angular momentum. If the medium is dense enough, then collisions between particles will be frequent, and the total angular momentum vector of two colliding particles will always be conserved. This allows a mechanism for a gas cloud to relax to its minimum energy state – an accretion disc.

As well as losing gravitational potential energy as it falls towards the central mass, a parcel of matter must always lose this angular momentum. Crucially, accretion discs provide a way for a given parcel of mass to lose angular momentum. If the disc itself maintains the same total angular momentum, then it follows that angular momentum must therefore be transported outwards.

1.1.2.1 Steady-state Accretion Discs: The α-prescription

The so-called α-disc model developed by (Shakura and Sunyaev 1973, hereafter SS73) and Lynden-Bell (1969) is currently the leading candidate for explaining how energy and angular momentum is transported an accretion disc. The starting point for this model is the parameterisation of viscosity using a simple form of

$$\nu = \alpha c_s H. \tag{1.9}$$

Viscous torques then allow the conversion of orbital kinetic energy into heat, which can be radiated away. If we then make one further assumption, that the accretion rate is constant throughout the disc, then we can write down a mass continuity equation valid at all radii, given by

$$\dot{M} \equiv 2\pi R V_R \Sigma = 0 \tag{1.10}$$

where Σ is the surface density at that point. The angular momentum equation becomes, in this case

$$\nu' \Sigma = \frac{\dot{M}}{3\pi}\left[1 - \left(\frac{R}{R_*}\right)^{1/2}\right] \tag{1.11}$$

The viscous torques throughout the disc cause a local loss of mechanical energy, allowing one to derive (see, e.g. Frank et al. 1992) a rate of viscous dissipation, per unit area, given by

$$D(R) = \frac{1}{2}\nu' \Sigma (R\Omega')^2. \tag{1.12}$$

Here, $D(R)$ is proportional to the derivative of the angular velocity, $\Omega' = d\Omega/dR$. By combining equations 1.12 and 1.11 we can show that the viscous dissipation rate is

$$D(R) = \frac{GM\dot{M}}{8\pi R^3}\left[1 - \left(\frac{R}{R_*}\right)^{1/2}\right] \tag{1.13}$$

where we have also set the angular velocity to the Keplerian velocity. This expression is, importantly, independent of viscosity – which is fortunate, because we do not know what value of α to use in equation 1.9. This result comes about because of the implicit assumption that the viscosity regulates the mass accretion rate so as to achieve a steady state.

We can now integrate across the whole disc to obtain the disc luminosity,

$$L_{disc} = 2\int_{R_*}^{\infty} D(R) 2\pi R dR = \frac{GM\dot{M}}{2R_*} = \frac{1}{2}L_{acc}. \tag{1.14}$$

This result can also be shown by considering the binding energy of gas at R_* and infinity. From equation 1.13 one can also derive an effective temperature distribution, by setting

$$\sigma T_{eff}^4(R) = D(R), \tag{1.15}$$

which then gives

$$T_{eff}(R) = T_* \left[1 - \left(\frac{R}{R_*} \right)^{1/2} \right]^{1/4}, \tag{1.16}$$

where

$$T_* = \left(\frac{3GM\dot{M}}{8\pi R_*^3 \sigma} \right)^{1/4}. \tag{1.17}$$

When $R >> R_*$ then we can simplify this to

$$T_{eff}(R) = T_* (R/R_*)^{-3/4}. \tag{1.18}$$

Now we have not only derived the total luminosity of an accretion disc, but also the effective temperature profile which will govern the shape of the emergent SED. This temperature profile is shown in figure 1.1 for the same four objects shown in table **??**, assuming an Eddington fraction of 0.2.

It is important to recognise that the steady-state disc treatment *does not specify the nature of the disc SED*. What it does do is say where energy is originally released. Typically, accretion discs are modelled as a series of annuli each emitting as blackbodies, but a disc atmosphere with frequency-dependent opacity would create a somewhat different spectrum. Figure ? shows the blackbody SEDs expected for the same objects as figure 1.1. Figure ? shows a comparison between a disc atmosphere model and blackbody model for a cataclysmic variable accretion disc, showing the differences in spectral shape caused by frequency-dependent opacities in the disc. It is of course possible that *neither* blackbody or disc atmosphere treatments are realistic. I shall therefore devote a little time to discussing the observational arguments for accretion discs and the different classes of accreting objects.

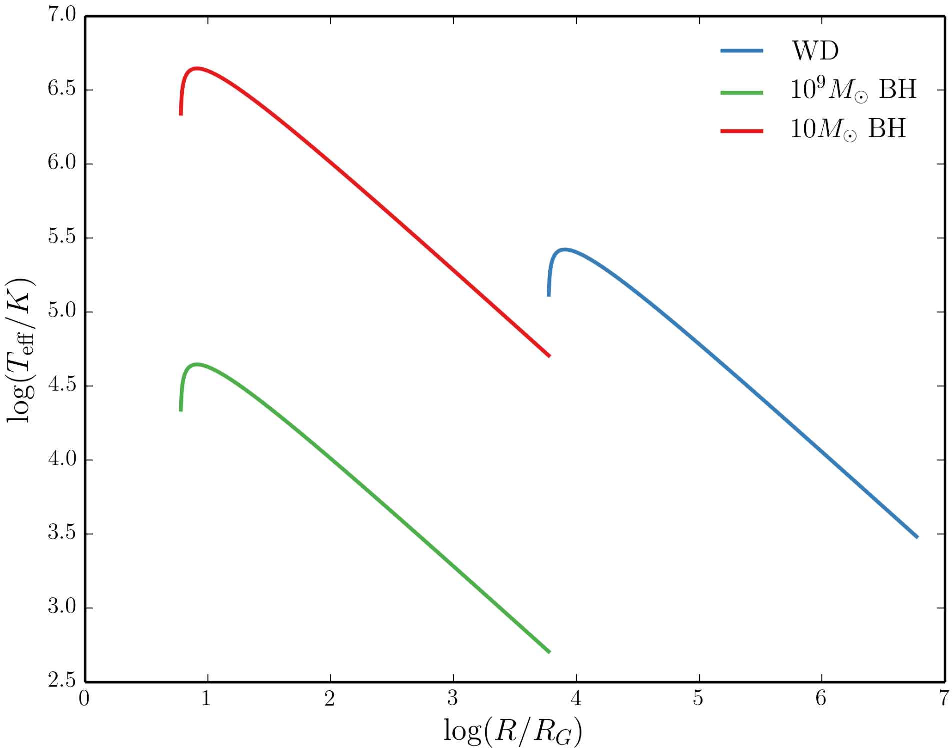

FIGURE 1.1: The temperature profile of an accretion disc for three different classes of compact object.

1.2 Accreting Compact Binaries

Accreting compact binaries form many different classes, but are all characterised by matter streaming from a donor star or secondary onto a compact object or primary. There are only two ways by which matter can transfer from the secondary to the compact object. One is by Roche Lobe-overflow (RLOF), whereby stellar evolution causes the donor star to fill it's Roche Lobe, the surface of equipotential around the star. The alternative is that the donor may expel material via a disc or radiatively driven stellar wind, allowing some of it to flow onto the compact object. Although accretion from a wind or circumstellar disc is common in high-mass X-ray binaries (HMXBs; e.g. Bartlett 2013), here I will focus on RLOF as it is more common in the systems that commonly exhibit high-state accretion discs and associated outflows. Two examples of these are shown in figure 1.2

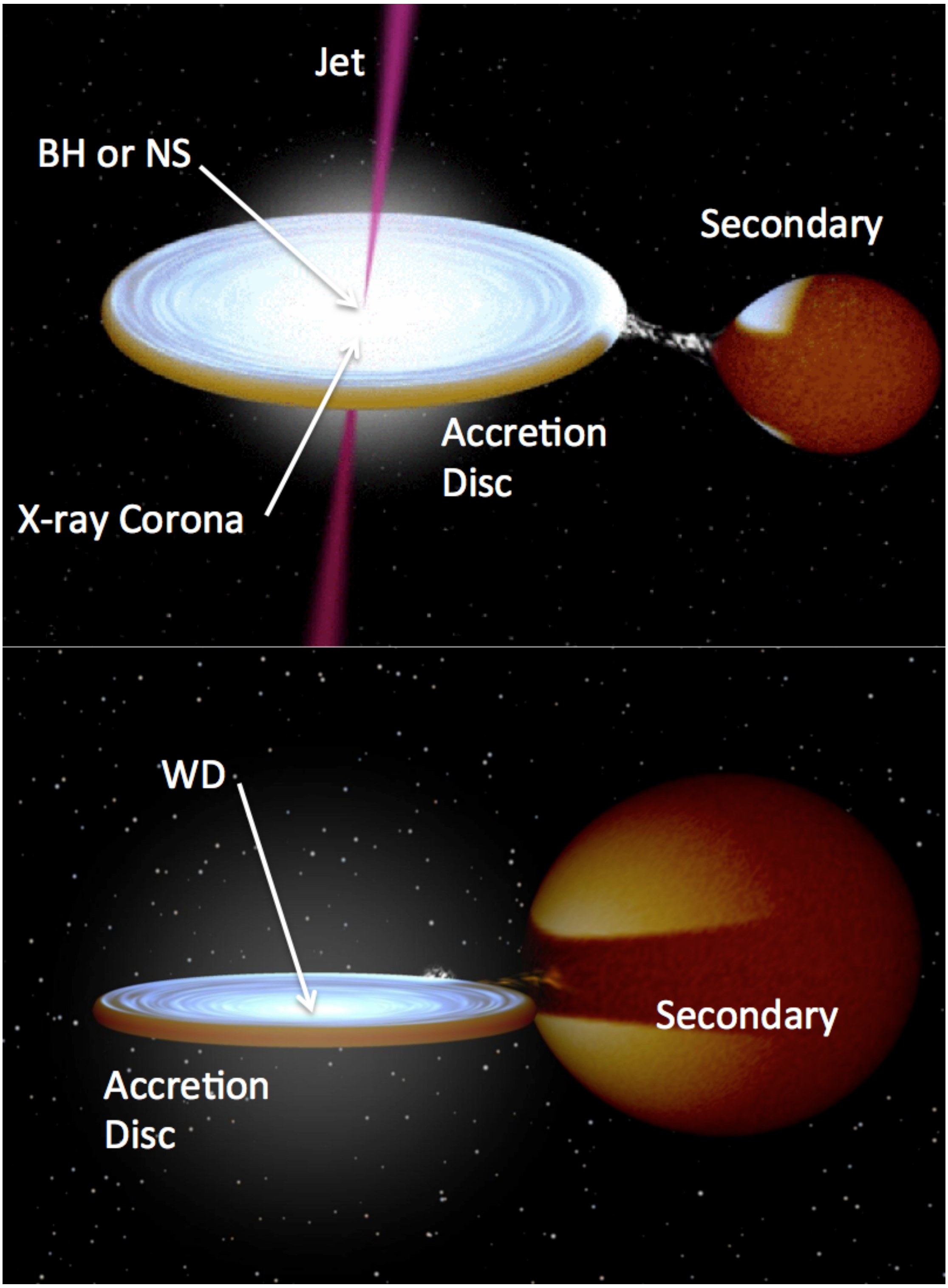

FIGURE 1.2: *Credit: Rob Hynes.* Artists impression of a low-mass X-ray binary (top) and cataclysmic variable (bottom). The key components are marked, and the clear similarity in overal structure is apparent.

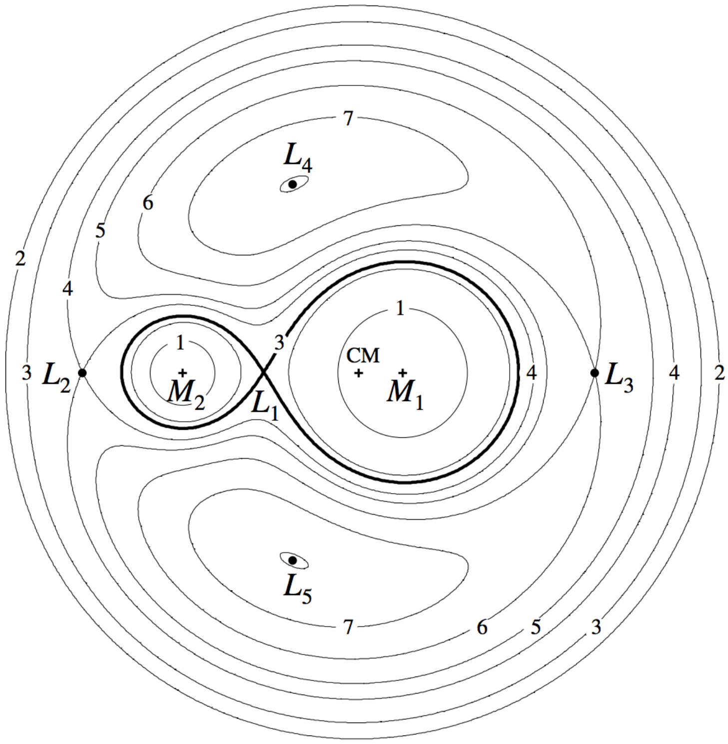

FIGURE 1.3: *Credit: Frank et al. 2002.* The Roche potential in a binary system for $q = M_2/M_1$ of 0.25. The Lagrangian points are marked, as are the locations of the individual and system centres of mass.

1.2.1 Roche Lobe-Overflow

Let us consider a binary system, with masses M_1 and M_2, at positions $\vec{r}_1$ and $\vec{r}_2$. The Roche potential, Φ_R, in this system is then

$$\Phi_R = -\frac{GM_1}{|\vec{r} - \vec{r}_1|} - \frac{GM_2}{|\vec{r} - \vec{r}_2|} - 1/2(\vec{\omega} \times \vec{r})^2, \tag{1.19}$$

where $\vec{\omega}$ is the angular velocity of the binary and is a vector normal to the orbital plane. This potential is plotted in figure 1.3 for a mass ratio, $q = M_2/M_1$ of 0.25.

In the context of semi-detached binary systems, the most important region of the potential is the dumbbell shaped region enclosing the masses. Each of these enclosed regions is known as the 'Roche lobe' of the object and can be expressed approximately in terms of the mass ratio and separation of the system. An approximation for the size of the Roche lobe takes the form (Eggleton 1983)

$$\frac{R_2}{a} = \frac{0.49q^{2/3}}{0.6q^{2/3} + \ln(1 + q^{1/3})}. \tag{1.20}$$

Here R_2 is the radius of a sphere with the same volume as the Roche lobe for the secondary star, which we can see depends only on q and the orbital separation, a. If this secondary expands enough to fill its Roche lobe, then matter will fall onto the other object. This process is known as Roche Lobe overflow (RLOF), and is vitally important in astrophysics. Although caused by stellar evolution, any accretion from RLOF will affect the mass ratio of the binary system and thus itself affects the evolution of binary systems. This helps determine the orbital period distribution of binaries (e.g. Knigge et al. 2011) as well as affecting the delay time distribution of Type Ia Supernovae, for which CVs are one of the progenitor candidates (e.g. Wang and Han 2012). It is also worth noting that the existence of gravitational waves has been required in models to explain the orbital period evolution of CVs since the 1960s (Kraft et al. 1962).

1.2.2 Cataclysmic Variables

Cataclysmic variables (CVs) are systems in which a WD accretes matter from a donor star via Roche-lobe overflow (see the 'CV bible', Warner 2003). CVs are not always dominated by their accretion luminosity; classical novae and super soft sources (SSS) emit mostly due to nuclear burning or detonation on the WD surface. Accretion dominated CVs – the focus here – can be classified according to the magnetic field strength (B) and photometric activity. Magnetic systems are classified as either 'Polars' ($B \gtrsim 10^7$ G) or 'Intermediate Polars' ($10^6 \lesssim B \gtrsim 10^7$ G); in these systems the accretion flow inside the some critical radius (related to the Alfven radius) is dominated by the WDs magnetic field (e.g. Patterson 1994). In polars this radius is large enough, due to the strong magnetic field, that no disc forms at all (Liebert and Stockman 1985). When $B \lesssim 10^6$ G then the accreting material can fall onto the WD via a disc, and the CV is classified as non-magnetic. There are a two main types of non-magnetic CVs; Dwarf Novae and Nova-like variables.

1.2.2.1 Dwarf Novae and the Disc-instability Model

Dwarf novae (DNe) are CVs that are characterised by repeated periods of quiescence and dramatic outburst. One of the most famous DNe is SS Cyg, whose light curve is shown in figure 1.4. The repeated outbursts can be clearly seen, and SS Cyg itself has been undergoing this behaviour for the full century for which it has been observed. A

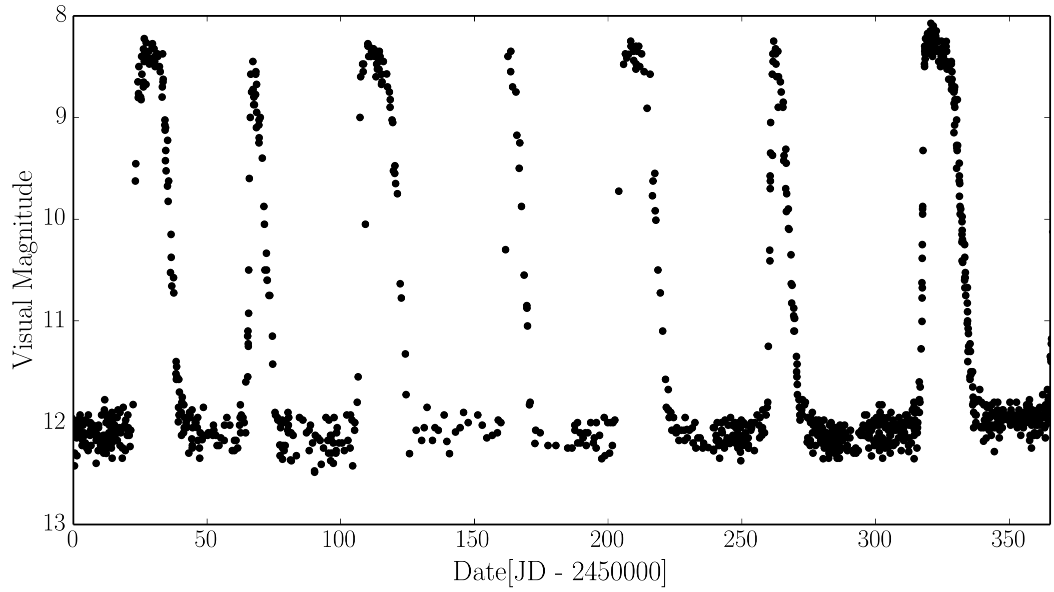

FIGURE 1.4: *Data: AAVSO.* A year in the life of SS Cyg, showing the characteristic repeated outbursts and periods of quiescence typical of a DN. SS Cyg has been undergoing this activity since it was first observed in 1896.

spectrum over the course of a typical outburst is shown in figure 1.5, and is characterised by the appearance of an optically thick accretion disc continuum – note the similarity to the stellar atmosphere disc spectrum computed in section 1.1.2.1, and to the intermediate inclination Nova-like variables discussed in the next section.

The leading candidate for explaining DN outbursts, and in fact the outbursts in low mass X-ray binaries or 'soft X-ray transients, is the disc-instability model (DIM; see Lasota 2001, and references therein). In this model, a gradual increase in supply rate from the donor star (and hence surface density in the disc) causes the disc to heat up. Eventually, the disc hits a critical temperature, around 7000 K, and becomes ionized. Now the surface density in the disc can increase significantly, and the disc becomes geometrically thin and optically thick. Most importantly, it can efficiently undergo radiative cooling, and a significant increase in brightness is observed.

1.2.2.2 Nova-like Variables

Nova-like variables (NLs) are similar to DNe, except that the disc is always in a relatively high-accretion-rate state ($\dot{M} \sim 10^{-8}$ M$_{\odot}$ yr^{-1}). NLs are therefore one of the best 'laboratories' for testing the steady-state accretion disc theory described in section 1.1.2.1. In the optical, NLs generally exhibit a series of H and He emission lines superposed

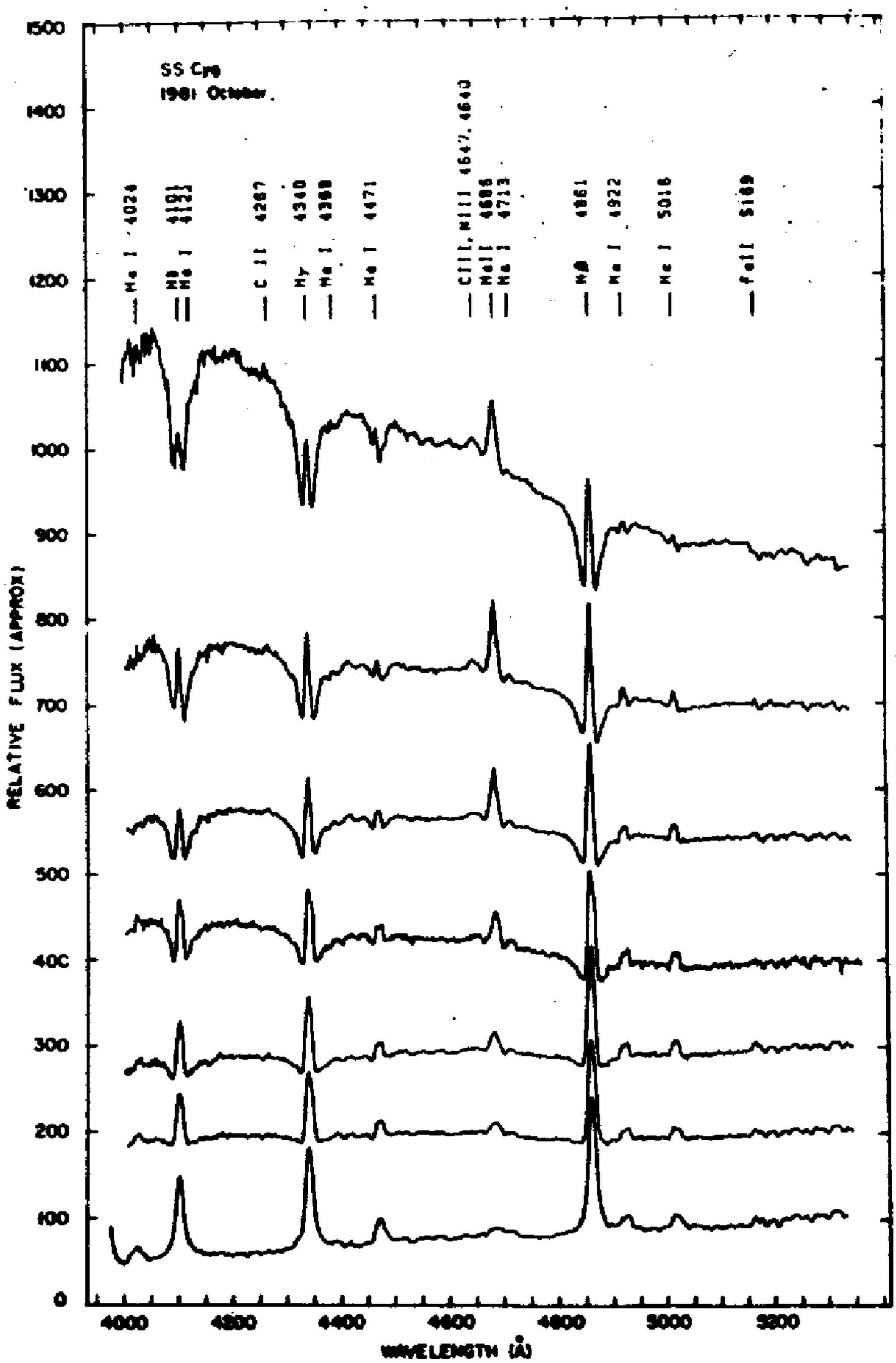

FIGURE 1.5: *Credit: Hessman et al. 1984 / Dhillon et al. 1996.* Spectra of SS Cyg during an outburst cycle, showing the evolution from minimum to maximum light. The rise is characterised by the appearance of an optically thick accretion disc spectrum. The flux scale is approximate.

on a blue continuum. In many cases, and particularly in the SW Sex subclass of NLs (Honeycutt et al. 1986; Dhillon and Rutten 1995), these lines are single-peaked. This is contrary to theoretical expectations for lines formed in accretion discs, which are predicted to be double-peaked (Smak 1981; Horne and Marsh 1986). *Low-state* CVs (dwarf novae in quiescence) do, in fact, exhibit such double-peaked lines (Marsh and Horne 1990).

1.2.3 Low Mass X-ray Binaries

Low Mass X-ray Binaries (LMXBs) are similar to CVs in structure (see figure 1.2), but the compact object is either a neutron star (NS) or black hole (BH). The accretion disc emits in the soft X-rays, and an additional hard X-ray power law is also seen in the spectrum (REFs). This hard component is normally attributed to Compton up-scattering of seed disc photons by some kind of 'corona' of hot electrons close to the BH (REFs). Although I do not study LMXBs directly in this thesis, it is instructive to discuss some of their observational appearance as it is relevant to the links between accretion and outflow. The discovery that XRBs follow similar tracks on a hardness-intensity diagram (REFs) is particularly interesting in this regard, especially since Ponti et al. (2012) showed that broad Fe absorption lines are only seen in the soft-state high-inclination systems (see section 2.1.2). This implies that equatorial outflows are intrinsic to the accretion process. Although the driving mechanism is almost certainly different to CVs (e.g. Díaz Trigo and Boirin 2015), the similarity in general structure to models for CVs and quasars is striking.

1.3 Quasars and Active Galactic Nuclei

Spectra of AGN have now been studied for over 100 years, and we have known that they exhibit strong, broad emission lines since the first spectrum was taken by Fath (1909). However, it wasn't until the work of Seyfert (1943) that the systematic classification of AGN really began, leading to the phrase 'Seyfert galaxy'. This label was applied to galaxies possessing a bright nucleus, spectroscopically characterised by a blue continuum and a series of strong emission lines. The first real physical insight into the extraordinary nature of AGN was provided by Woltjer (1959), who noted that (i) the nuclei must have

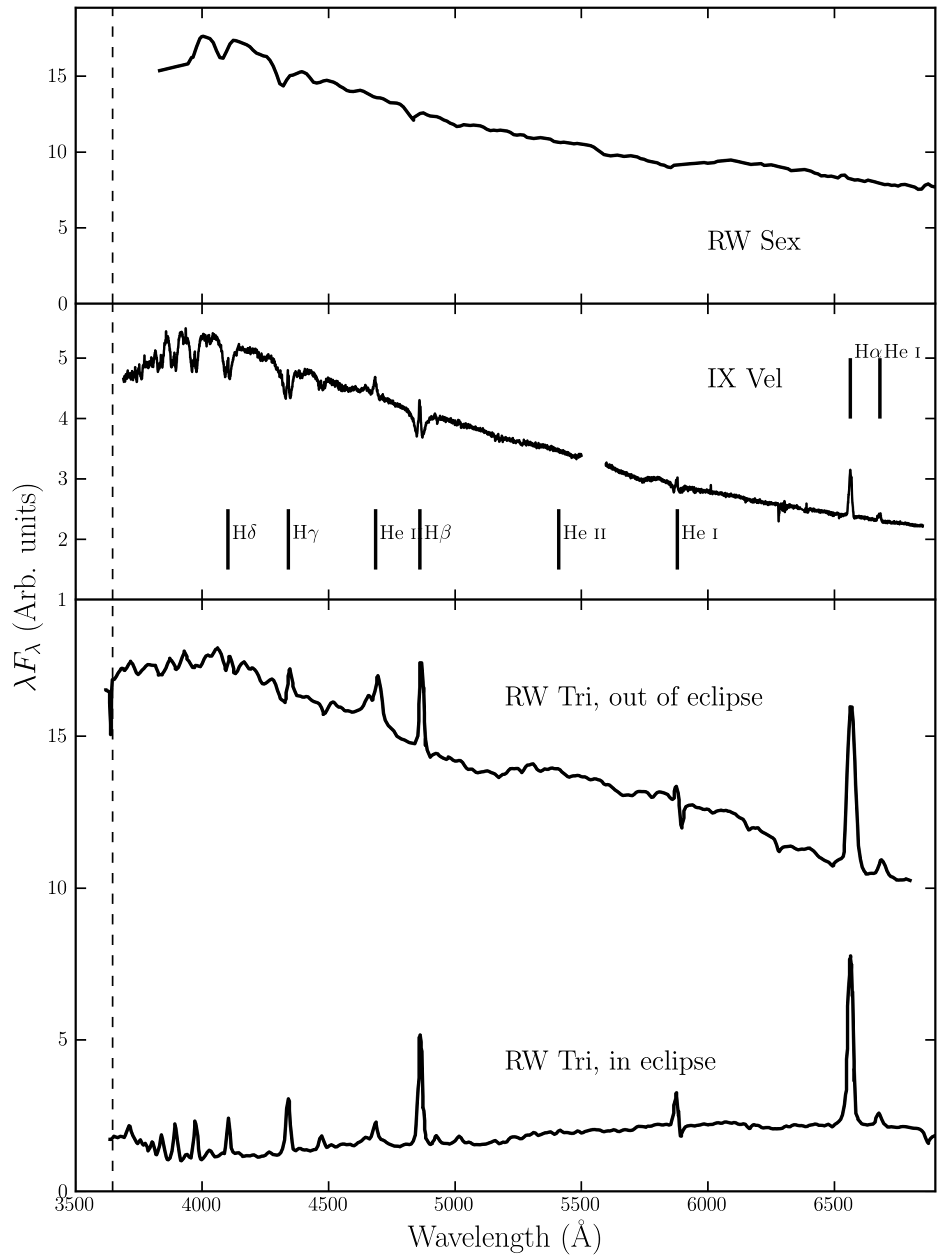

FIGURE 1.6: Optical spectra of three nova-like variables.

sizes < 100 pc, based on the fact that they were unresolved and (ii) the mass of the nucleus must be very high, based on virial arguments. While both of these observations were based on simple arguments, the fact that these ultra-luminous celestial objects are both *compact* and *supermassive* is perhaps the defining insight into the nature of AGN.

Although the field of AGN study was established in the optical, radio astronomy also significantly furthered our understanding of AGN in the mid-20th century. A number of surveys, such as the Cambridge (Edge et al. 1959), Parkes (Ekers 1969) and Ohio (Ehman et al. 1970) surveys discovered a great many bright radio point sources distributed isotropically across the sky. These sources eventually became known as 'quasi-stellar radio sources' or *quasars*, and were soon identified to be coincident with bright optical sources or 'quasi-stellar objects' (QSOs; REFs). Nowadays, the term quasar normally has very little to do with radio emission and is often used interchangeably with QSO. Indeed, throughout this thesis I shall refer to a quasar as simply a bright, massive AGN; one with sufficiently high luminosity that it dominates the emission from it's host galaxy.

One of the main classifications schemes for AGN is a spectroscopic one, based on whether an object possesses broad emission lines in its spectrum, such as C IV broad Hβ and Lyα, in addition to the narrow lines that are always present. If these broad lines are seen, then the AGN is classed as type I, and if not, it is a type II; example spectra are shown in figure 1.7. These designations were originally applied to Seyfert galaxies (Seyfert 1943), but can also be used to classify the more luminous quasar class, despite the apparent difficulty in finding the expected number of type II sources (Zakamska et al. 2003). These classifications are complicated somewhat by narrow line Seyfert Is, which may be explained by super-Eddington accretion (Done and Jin 2015) or perhaps simply an orientation effect (Baldi et al. 2016), and the so-called 'true type II' AGN, in which the broad line region is absent (Tran 2001; Shi et al. 2010) rather than obscured (see next section). Despite the muddying of the waters, what was originally a clear dichotomy in spectral type provided a profound motivation for attempting to *unify* AGN via geometric arguments.

1.3.1 AGN Unification and the dusty Torus

Although Seyfert had identified type 1 and 2 AGN, a physical explanation for this dichotomy was not forthcoming until a study by (Antonucci and Miller 1985, AM85).

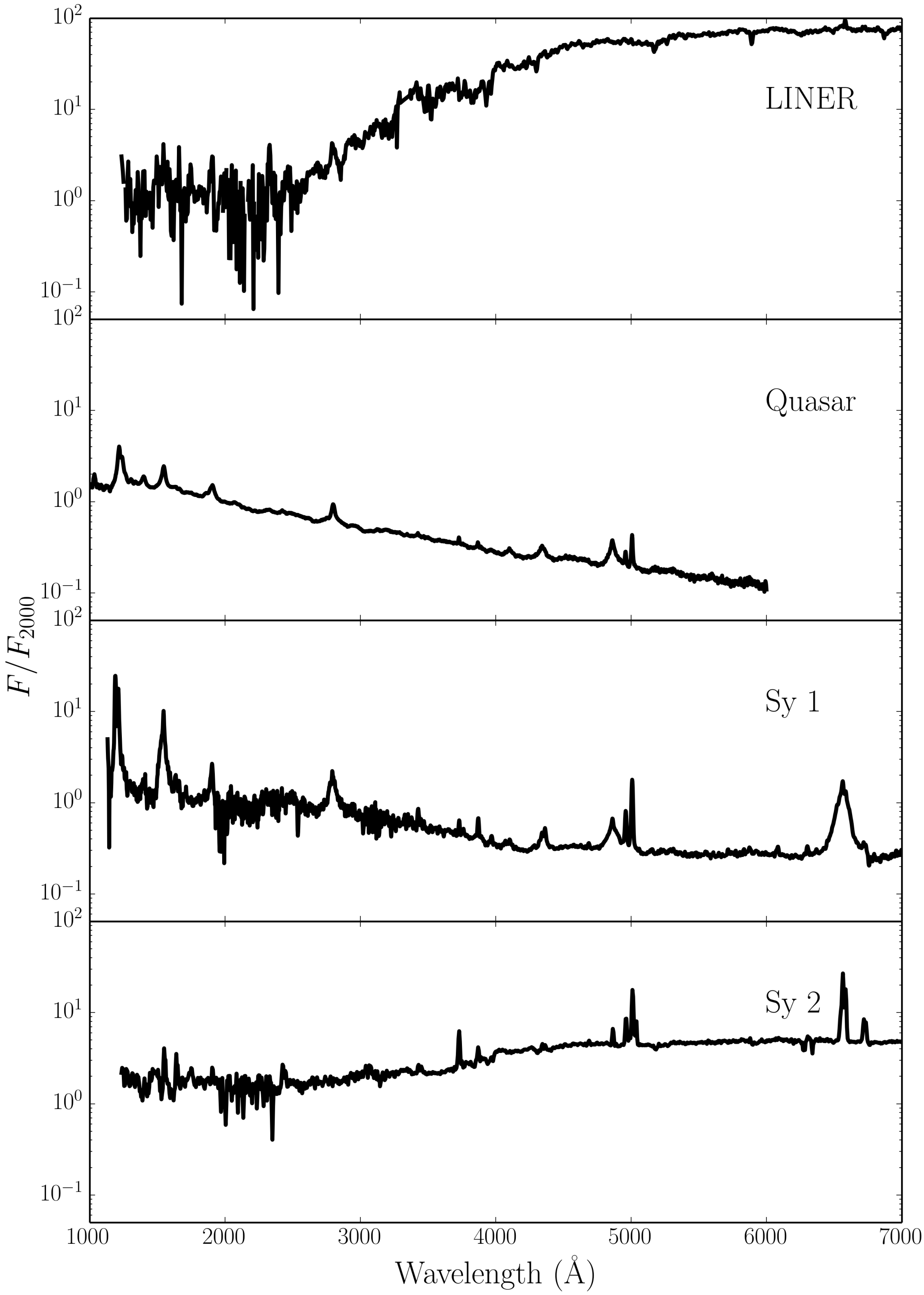

FIGURE 1.7: Template spectra, from the AGN atlas, for four common types of AGN. Obtained from http://www.stsci.edu/hst/observatory/crds/cdbs_agn.html.

They showed unambiguously that the nearby Seyfert 2 NGC 1068 is simply an obscured type 1 AGN, by finding that broad emission lines appeared in the spectrum of *polarised* flux. This provided the basis for the first successful attempt to unify AGN behaviour, as it elegantly explained the apparent disconnect between the two types of AGN as simply a viewing angle effect; at one angle, you could look directly into the broad line region (BLR) near the nucleus, but at Type 2 angles this region was hidden from view. The obscuring structure became known as the 'torus' (Krolik and Begelman 1986), due to its geometry, and it was soon realised that this structure may be made of dust, in which case it could also be responsible for the infra-red (IR) bump in AGN (Neugebauer et al. 1979).

(Urry and Padovani 1995, UP95) went further than the original unification model proposed by AM85 as they also tried to explain radio AGN phenomena. The picture they proposed is shown in figure 1.8. This model attempts to explain all of the types of AGN described in section **??** merely as a function of viewing angle and presence, or lack thereof, of a radio jet. Models such as this also describe the series of 'bumps' observed in AGN – the portions of the spectrum that dominate the luminosity, shown in figure 1.9. In most models, the 'Big Blue Bump (BBB)' is ascribed to thermal emission from an accretion disc, and the 'Small Blue Bump' to optically thin Balmer continuum and Fe II emission from the BLR. The latter can just be seen between ~ 2000Å and ~ 4000Å in the Seyfert 1 and quasar templates in figure 1.7. Our understanding of the BBB is still unsatisfactory (see section 1.4).

Since the seminal works by AM85 and UP95, the picture has become somewhat more complicated. Variable X-ray absorption has been detected in so-called 'Changing look' AGN (Matt et al. 2003; Puccetti et al. 2007), even in NGC 1068 itself (Marinucci et al. 2016). Changes in type have also been seen in the optical lines; the broad Hβ component can dramatically disappear or reappear (e.g. Tohline and Osterbrock 1976; Cohen et al. 1986; Denney et al. 2014). The explanation for this could be variable absorption (Elitzur 2012) or linked to the accretion state of the disc. In the latter case, it has even been suggested that a disc wind could be directly responsible for this change in accretion state (Elitzur et al. 2014). Furthermore, dusty *polar* outflows have been found to be important IR emitters (Hönig et al. 2013), implying that, even when it comes to dust, the torus is not the whole picture. Despite these complications, the AGN torus unification picture

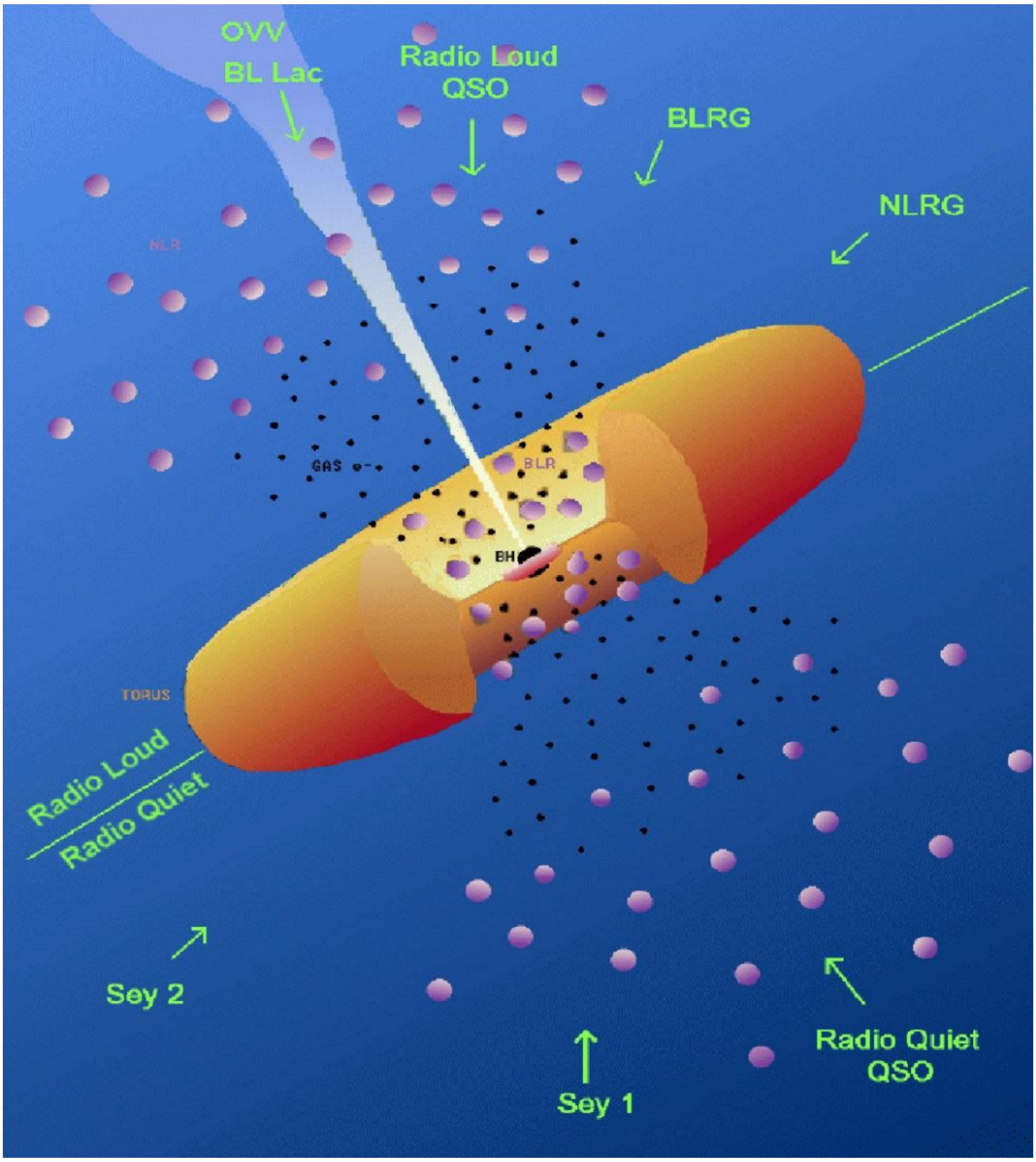

FIGURE 1.8: A unified scheme for AGN.

still helps explain a lot of AGN behaviour, and represents a good framework to test with observations.

1.3.2 X-ray Properties of AGN

Approximately 10% of the bolometric luminosity of AGN comes out in the X-ray band between $\sim$ 0.1 and $\sim$ 100 keV. Thus, AGN dominate the cosmic X-ray background (Madau et al. 1994). The hard X-ray emission follows a typical power law shape with spectral index ?? (REFs), widely considered, as in LMXBs, to come from a hot 'corona'

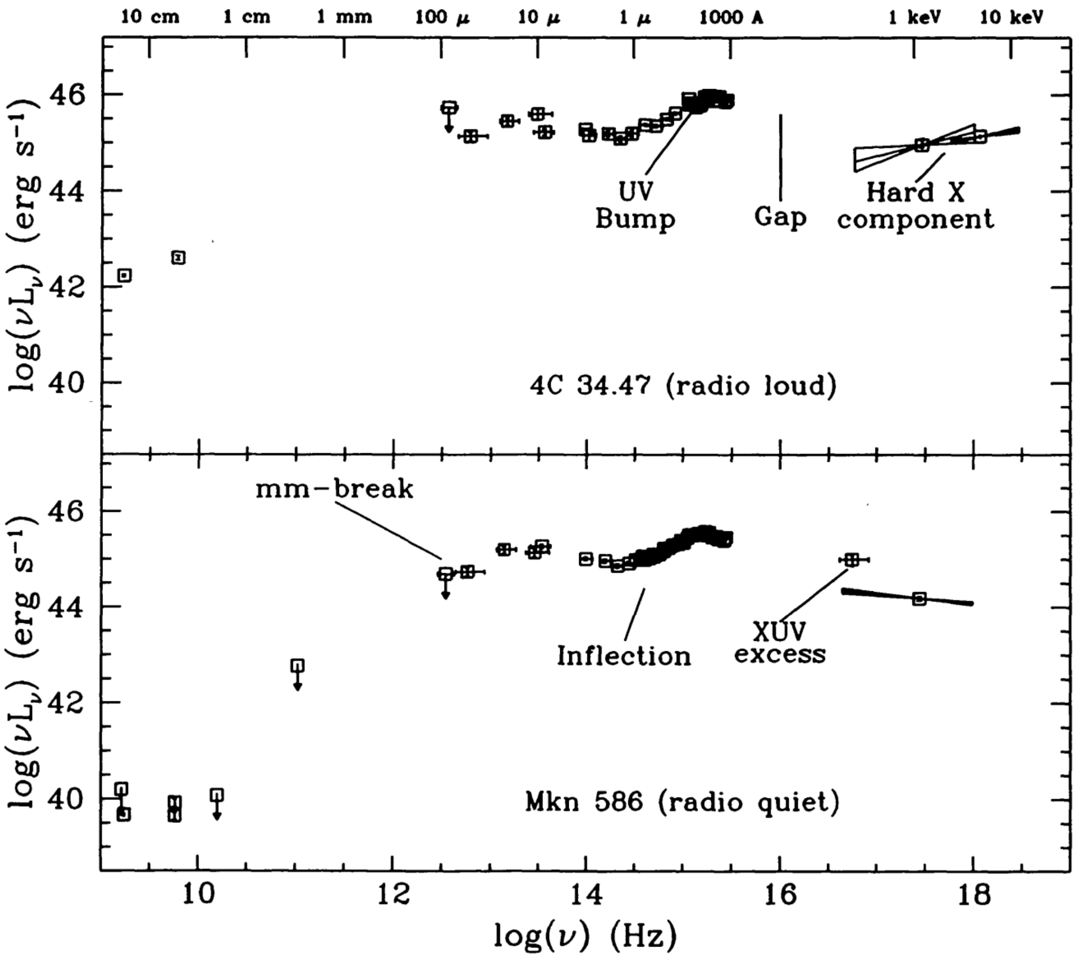

Figure 1.9: Radio-loud (top) and radio-quiet (bottom) quasar SEDs from Elvis (1994). The UV bump is the BBB, and the IR bump can clearly be seen. The XUV or Soft-X-ray excess is also visible in the radio-quiet panel (see section 1.3.2.1).

of electrons, close to the BH, that upscatters disc seed photons (e.g. Haardt and Maraschi 1991). The compactness of this X-ray corona has been recently confirmed with microlensing (REFs) and variability studies (REFs). X-rays in AGN can be highly variable, both in terms of their intrinsic X-ray emission (REFs) and due to changes in the absorption characteristics (REFs). I discuss absorption in more detail, particular with respect to winds, in section ?.

1.3.2.1 The Soft X-ray Excess

If one extrapolates the $\nu^{-1/3}$ law from the BBB, and the power law in the hard X-rays, a curious excess of flux is often found in the soft X-rays in type 1 AGN (see figure 1.9, from Elvis et al. 1994). This is known as the soft X-ray excess (SXXS), which is too hot to be explained by thermal disc emission, as a thin disc around an AGN should never approach the temperatures required. Many models have been proposed to explain this excess, including relativistically smeared photoabsorption (Gierliński and Done 2004, 2006), relativistically smeared line and free-free emission (Ross and Fabian 2005) and a variety of cool Comptonised component geometries such as an inner accretion flow (Magdziarz et al. 1998; Done et al. 2012) and thin layer on top of the disc (Janiuk et al. 2001). While the SXXS poses challenges to the simplest pictures of AGN, it may also solve some of the issues, as some of the geometries proposed may help explain the accretion disc size problem (Done, private communication; see section 1.4) or inability to match observed spectra.

1.3.3 The Broad Line Region and Connection to Outflows

In the UP95 unification model, the broad emission lines come from a series of virialised clouds close to the disc plane. As noted by (Murray et al. 1995, hereafter MCGV95), there are a number of problems with the BLR 'cloud' model, perhaps most notably that there is no obvious physical origin for a series of virialised clouds. Testing alternative models for the BLR is therefore important. Indeed, MCGV95 proposed a disc wind model in order to explain both BALs and BELs in quasars. A disc wind model was also discussed by Elvis (2000), who proposed a structure for quasars that attempted to explain much of the behaviour of luminous AGN merely as a function of viewing angle. Outflow models are discussed further in section 2. The philosophy of these models is that, before invoking additional degrees of freedom in a model, we should first test if known quasar phenomenology (winds) can explain other aspects of their observational appearance. I have illustrated this general principle with the 'Occam's quasar' cartoon shown in figure 1.10. This is the picture that I will quantitatively test in the latter, quasar-focused sections of this thesis, and the general principle can even be applied to cataclysmic variables and other accreting objects.

1.4 The Current Understanding of the Disc Continuum

The SS73 model is still the most common way to fit accretion disc spectra and infer information about the underlying physics. However, a number of issues have been raised

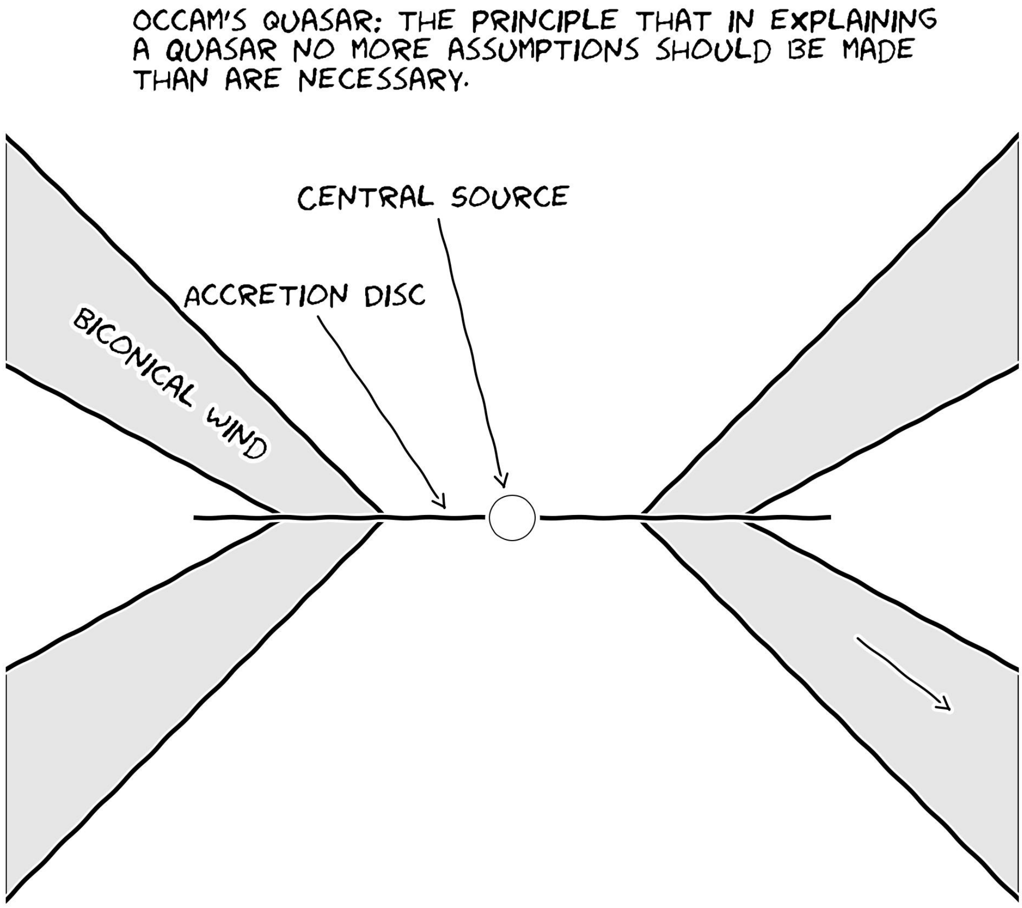

Figure 1.10: Occam's quasar. How far can this general picture take us when trying to explain the behaviour of quasars and other accreting compact objects?

with the thin-disc model and its applicability to accreting systems.

1.4.1 The Spectral shape of CV discs

Attempts to fit the observed SEDs of high-state CVs with simple disc models have met with mixed success. In particular, the SEDs predicted by most stellar/disc atmosphere models are too blue in the UV (Wade 1988; Long et al. 1991, 1994; Knigge et al. 1998a) and exhibit stronger-than-observed Balmer jumps in absorption (Wade 1984; Haug 1987; La Dous 1989; Knigge et al. 1998a). One possible explanation for these problems is that these models fail to capture all of the relevant physics. Indeed, it has been argued that a self-consistent treatment can produce better agreement with observational data (e.g. Shaviv et al. 1991; but see also Idan et al. 2010). However, an alternative explanation, suggested by Knigge et al. (1998b; see also Hassall et al. 1985), is that recombination continuum emission from the base of the disc wind might fill in the disc's Balmer absorption edge and flatten the UV spectrum.

Alternatively, it may just be that CV disks are never really in a steady state, and so we should only expect the $R^{-3/4}$ temperature profile to hold in a limited portion of the disc. From eclipse mapping, it has been shown that the inferred accretion rate increases with radius in NLs (Rutten et al. 1992; Horne 1993). These results suggest that a non-radiative form of energy loss is present in the inner regions of the disc, of which potential forms would be advection or mass loss. This is yet another piece of evidence that the understanding of accretion and outflow are intertwined, although hopefully not inextricably.

1.4.2 The Big Blue Bump in AGN

Does the SS73 model apply well to AGN spectra? There are constrasting views on the matter. On the one hand, Antonucci (2013) claims that "Most of the AGN community is mesmerized by unphysical models that have no predictive power". Yet a recent spectral fitting study by Capellupo et al. (2015) concludes that "Altogether, these results indicate that thin ADs are indeed the main power houses of AGN". So, what are the current problems when confronting thin disc models with observation?

1.4.2.1 Fitting AGN Spectra

1.4.2.2 The 1000Å Break

1.4.2.3 The Accretion Disc Size Problem

One of the most interesting results of recent years relating to AGN and accretion discs is the discovery that the continuum emission region size is a factor ~ 3 larger than predicted by standard thin disc theory. This result has been found independently in both microlensing (Morgan et al. 2010) and reverberation (Edelson et al. 2015), and poses a challenge to the current best-bet model for the big blue bump in AGN. One proposed solution is that the discs in AGN are inhomogenous, consisting of individual clumps with independently varying temperatures (Dexter and Agol 2011), but this is very much still an active area of research. It is worth noting that the impact of winds on these results has not yet been properly quantified, something our team is currently trying to address (Mangham et al. prep)

1.5 The Universality of Accretion

Accretion appears to be an important physical processes across ~ 10 orders of magnitude in mass. But is this process the same at all scales? Does any behaviour manifest in all accretion systems?

1.5.1 The RMS-flux relation

Broad-band variability is common in all types of accretion disc. It has been known for some time that there exists a linear relationship between the flux and absolute root-mean-square (rms) amplitude of this variability. This was discovered first in XRBs and AGN (Uttley and McHardy 2001; Uttley et al. 2005; Heil et al. 2012), but it has been shown more recently that the relationship extends to CVs and even YSOs (Scaringi et al. 2012, 2015). The relationship is not limited to one type of CV, as it is present in both NLs and DNe (Van de Sande et al. 2015).

The model that best reproduces this behaviour is the so-called 'fluctuating accretion disc' model (Lyubarskii 1997; Kotov et al. 2001; Arévalo and Uttley 2006; Hogg and Reynolds 2015). It has been shown that additive processes cannot reproduce the behaviour, and a multiplicative mechanism is required (Uttley et al. 2005). Regardless of the mechanism, the rms-flux relation is one of the most clear-cut examples of a universal accretion phenomenon. It tells us that at least some of the behaviour in CV discs is present in AGN and XRBs, strengthening the argument that CVs should be used as 'accretion laboratories'.

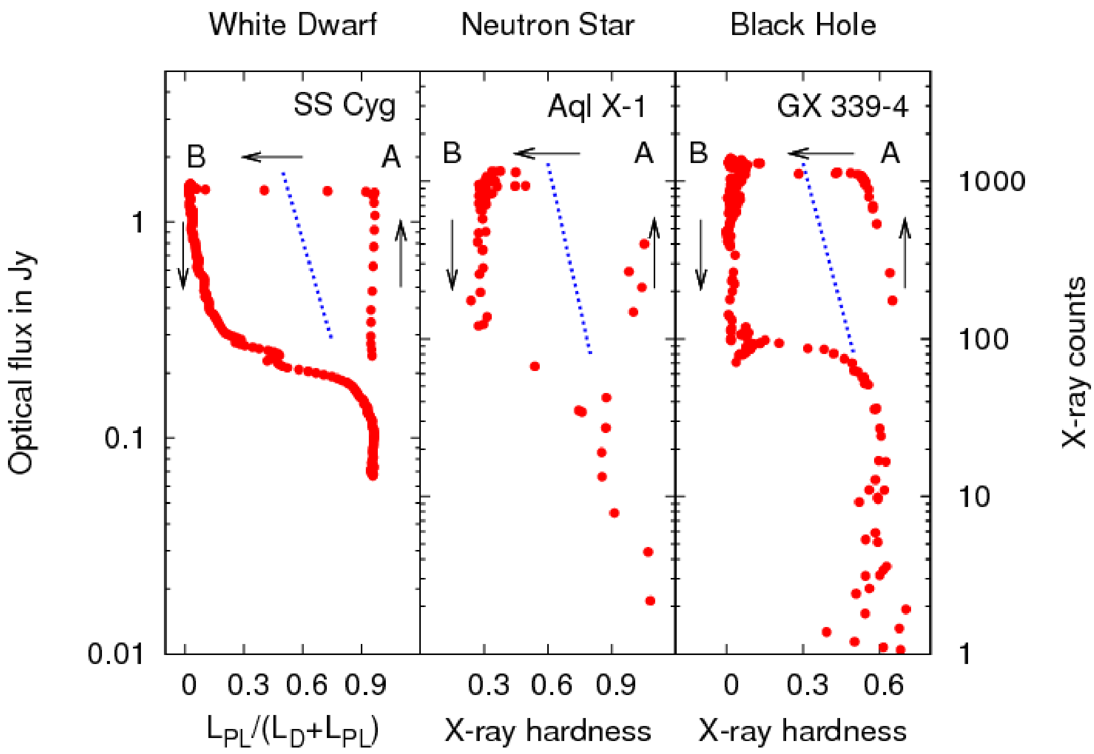

FIGURE 1.11: *Credit: Kording et al. XXXX.* Caption.

1.5.2 Accretion States

1.5.3 Jets and Outflows

1.5.4 A Global Picture

Clearly, accretion physics is relevant to a plethora of astrophysical phenomena, and at least some of the physics of accretion is applicable to *all* classes of accreting object. It would also appear that the outflowing material observed in accreting systems has a profound effect on the accretion process itself, and possibly significantly affecting the observational appearance of accretion discs (c.f. Elvis unification model). Hence, in the next chapter, I will detail the evidence for winds and discuss some of their theoretical considerations.

Chapter 2

Accretion Disc Winds

> "A view of space, with an elephant
> obstructing it"
> *Mike Vennart, Silent/Transparent*

2.1 Observational Evidence

The observational evidence for mass-loaded outflows or winds is widespread across the entire astrophysical mass range and most of the electromagnetic spectrum. Before detailing the more compelling aspects of this evidence, it is pertinent to briefly discuss the 'smoking gun' used to unambiguously detect winds – the presence of blue shifted BALs or 'P-Cygni' profiles in an objects spectrum.

Figure ?? shows how a spherical outflow of significant opacity will cause these characteristic line profile shapes to form, as scattering out of the line of sight causes a dip in the blue wing of the line, while scattering into the line of sight from other portions of the outflow causes an increase in flux in the red wing of the line. The situation is much more complex in most astrophysical situations; for example, the geometry is rarely spherically symmetric, and the line is rarely a pure scattering case. Indeed, the potential for complicated radiative transfer effects and variety in line formation mechanisms is one of the reasons why 3D Monte Carlo radiative transfer simulations are necessary to effectively model disc winds (see section 3).

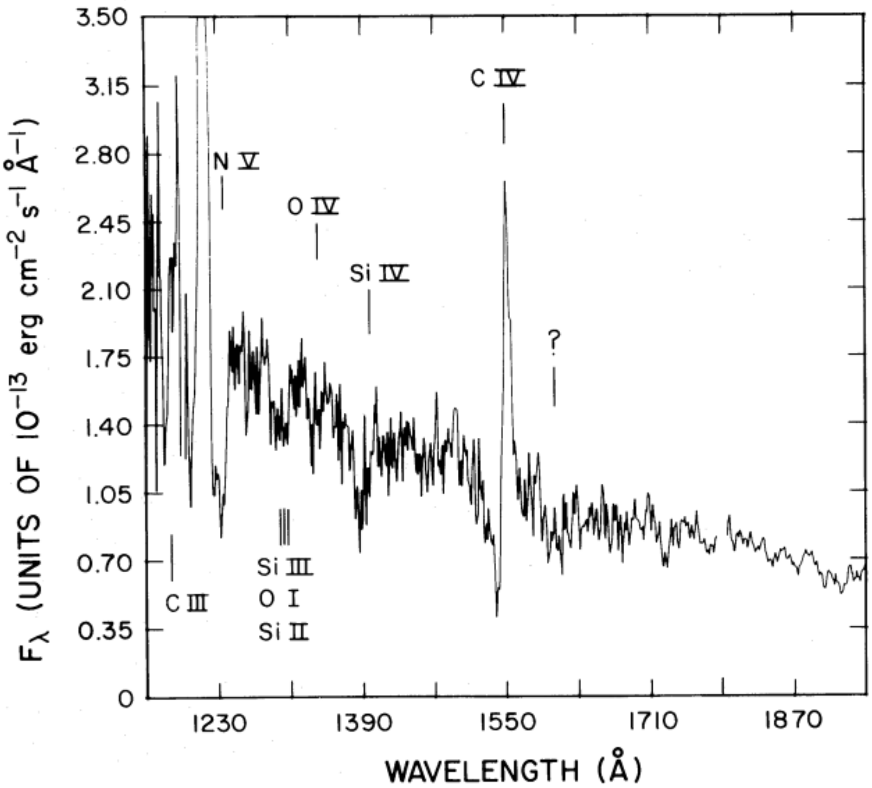

FIGURE 2.1: *Credit: Cordova & Mason 1982.* UV spectrum of the DN TW Vir during outburst. The P-Cygni profiles can be seen clearly, demonstrating that a strong, fast outflow is present in the system.

2.1.1 Cataclysmic Variables

It has been known for a long time that winds emanating from the accretion disc are important in shaping the ultraviolet (UV) spectra of high-state CVs (Heap et al. 1978; Greenstein and Oke 1982). The most spectacular evidence for such outflows are the P-Cygni-like profiles seen in UV resonance lines such as C IV $\lambda1550$ (Cordova and Mason 1982, ; see figure 2.1)). Considerable effort has been spent over the years on understanding and modelling these UV features (e.g. Drew and Verbunt 1985; Mauche and Raymond 1987; Shlosman and Vitello 1993; **?**; Knigge and Drew 1997; Knigge et al. 1997; Long and Knigge 2002; Noebauer et al. 2010; Puebla et al. 2011). The basic picture emerging from these efforts is of a slowly accelerating, moderately collimated bipolar outflow that carries away $\simeq 1\% - 10\%$ of the accreting material. State-of-the-art simulations of line formation in this type of disc wind can produce UV line profiles that are remarkably similar to observations, as shown in figure 2.2.

Much less is known about the effect of these outflows on the optical spectra of high-state

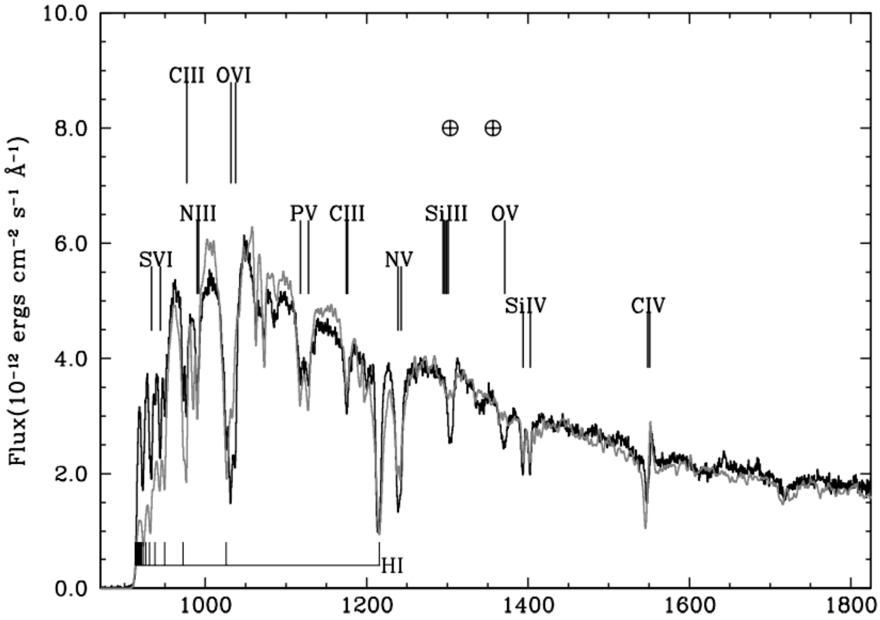

FIGURE 2.2: *Credit: Long & Knigge 2002.* UV spectrum of Z Cam, compared to a synthetic spectrum from MCRT simulations.

CVs. Direct evidence of wind-formed lines comes from isolated observations of P-Cygni-like line profiles in Hα and He I λ5876, (Patterson et al. 1996; Ringwald and Naylor 1998; Kafka and Honeycutt 2004). However, the effect on the *emission* aspects of the optical spectrum is not well known. Murray and Chiang (1996, 1997) have shown that the presence of disc winds may offer a natural explanation for the single-peaked optical emission lines in high-state CVs, since they can strongly affect the radiative transfer of line photons (see figure ??). Stronger support for a significant wind contribution to the optical emission lines comes from observations of eclipsing systems. There, the single-peaked lines are often only weakly eclipsed, and a significant fraction of the line flux remains visible even near mid-eclipse (e.g. Baptista et al. 2000; Groot et al. 2004). This points to line formation in a spatially extended region, such as a disc wind (see section **??**). It is also possible that a wind may affect the continuum emission of CVs, as described in section ??. The effect of an accretion disc wind on the optical line and continuum emission of CVs is addressed directly, via radiative transfer modelling, in chapter 4.

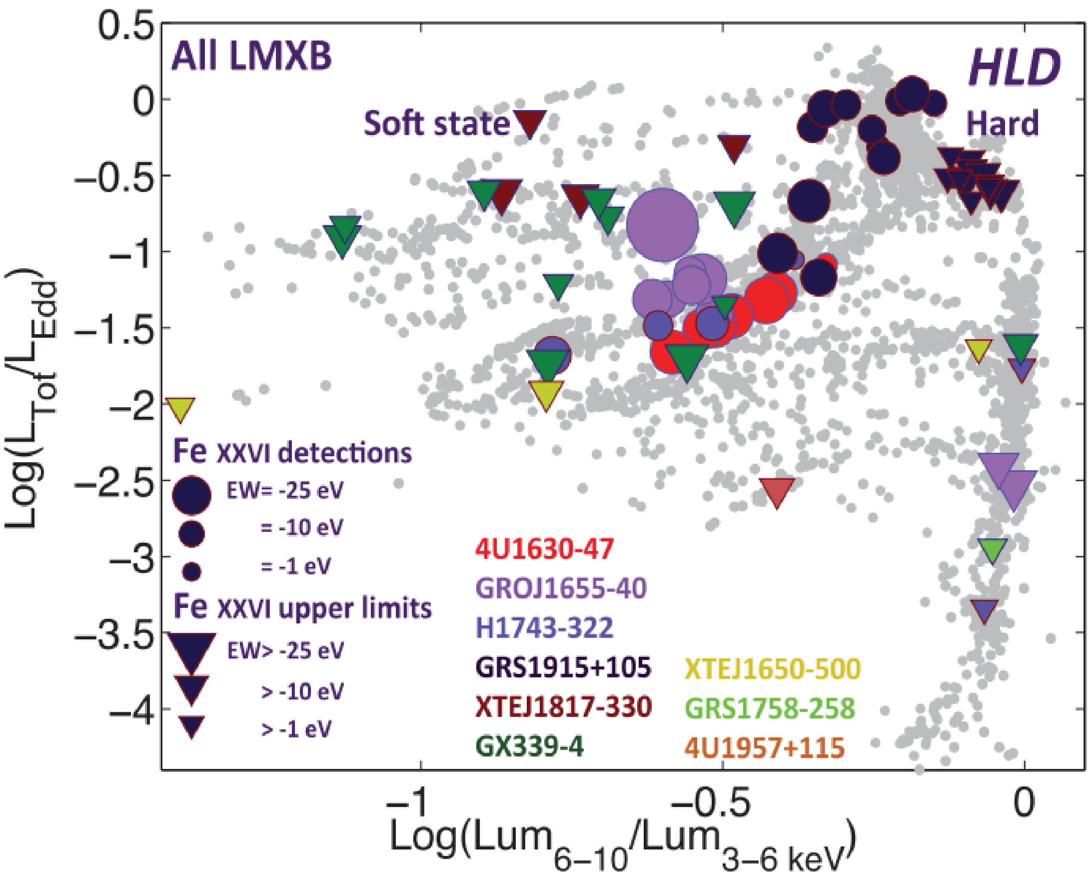

FIGURE 2.3: *Credit: Ponti et al. 2012.* HID demonstrating that winds appear in the soft states of LMXBs.

2.1.2 X-ray Binaries

Like CVs, evidence for fast outflows in LMXBs is not constrained to a single waveband. UV absorption in outflows was detected when Ioannou et al. (2003) observed C IV λ1550 P-Cygni profiles with blueshifts of ∼ 1500km s^{-}1. Shortly after, a series of papers found highly ionized Fe absorption with similar blueshifts and FWHM of around 1500km s^{-}1 (REFs). These absorption features tended to be detected in high-inclination, 'dipping' LMXBs, and this was confirmed in more sources by Ponti et al. (2012), who proposed an equatorial geometry based on this (see figure ??). The same study demonstrated (figure ??) that the winds only appeared in the soft, disc dominated accretion state, on the opposite side of the HID to the region where jets are common. This exciting result demonstrated how important winds are to our understanding of accretion, and required that we expand the discussion of accretion states to include 'disc-jet-wind' coupling.

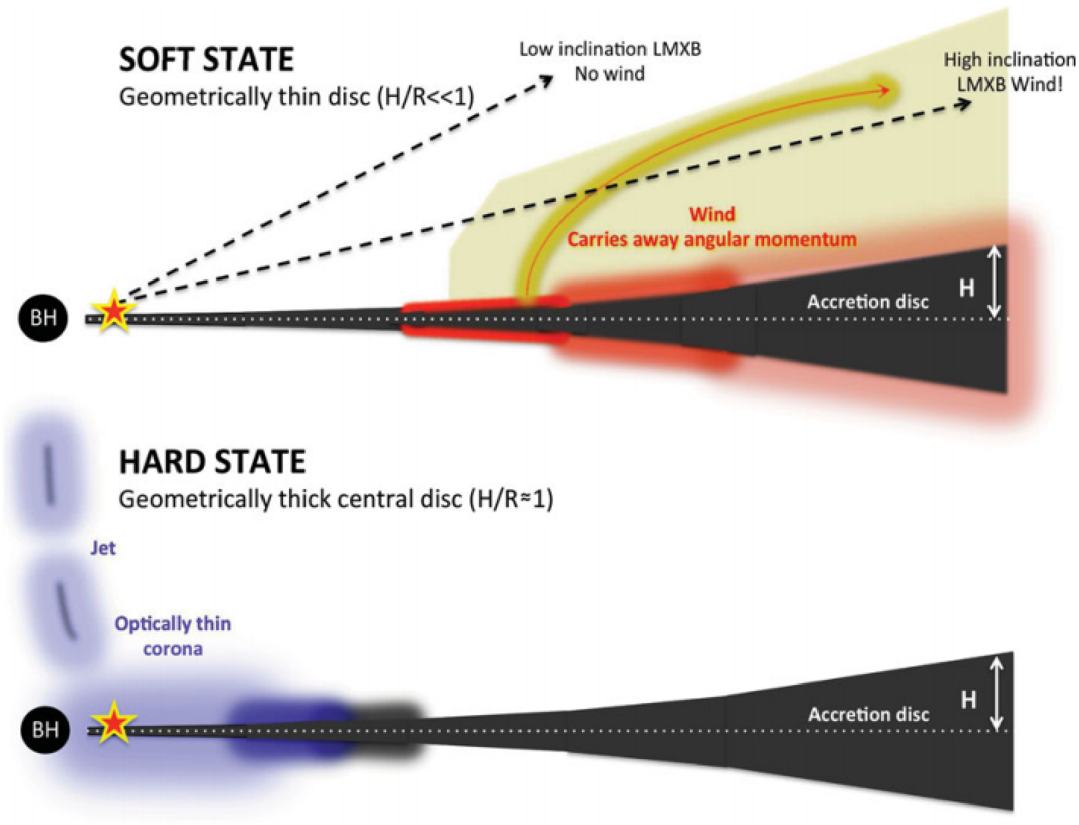

FIGURE 2.4: *Credit: Ponti et al. 2012.* A cartoon illustrating the expected geometry of soft-state LMXB winds.

2.1.3 AGN and Quasars

2.1.3.1 Broad Absorption Line Quasars

2.1.3.2 Warm Absorbers

2.1.3.3 Ultra-fast Outflows

2.1.4 Stellar Winds

Although stellar winds are clearly not accretion disc winds, they provide a useful, and better understood, testing ground for much of the physics of radiatively-driven outflows.

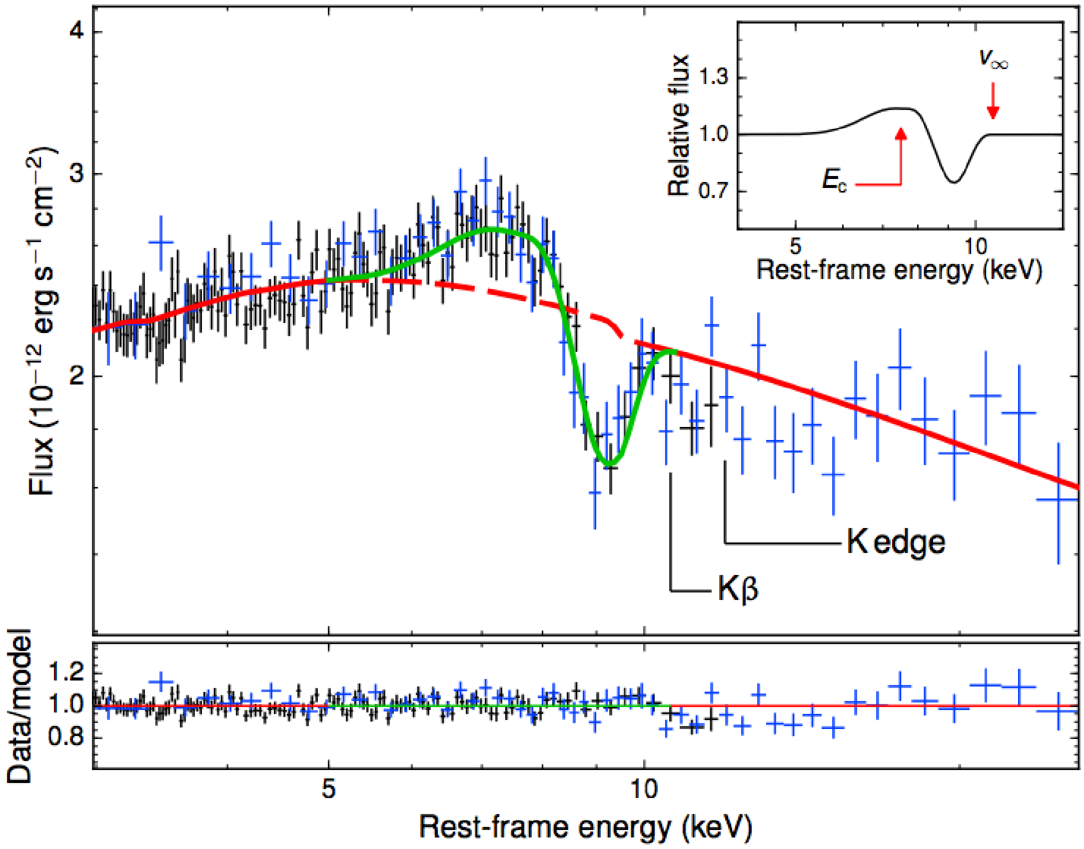

FIGURE 2.5: *Credit: Nardini et al. 2015.* X-ray spectrum fitted with a P-Cygni profile from a spherical outflow model. *XMM-Newton* data is shown in black with two combinaed *NuStar* observations in blue.

2.1.4.1 Clumping

2.2 Driving Mechanisms

Let us consider a parcel of ideal gas. By imposing nothing more than conservation of mass, energy and momentum on that parcel we can write down three equations of hydrodynamics [1]

$$\frac{D\rho}{Dt} + \rho\nabla \cdot \vec{v} = 0 \tag{2.1}$$

$$\rho\frac{Dv}{Dt} = -\nabla P + \frac{1}{4\pi}(\nabla \times \vec{B}) \times \vec{B} + \rho\vec{F}_{rad} + \rho\vec{g} \tag{2.2}$$

[1] I stress that these equations are not used in hydrodynamic simulations in this thesis (see section ?, for example); they are discussed here because they provide a natural reference point for exploring potential driving mechanisms for winds in accreting systems.

$$\rho \frac{D}{Dt}\left(\frac{e}{\rho}\right) = P\nabla \cdot \vec{v} + \rho\mathcal{L} \tag{2.3}$$

Here D denotes a derivative within the comoving frame of the gas parcel, $\vec{v}$ is the velocity, ρ is the gas density, $\vec{B}$ is the local magnetic field, $\vec{F}_{rad}$ is the radiation force per unit mass and $\vec{g}$ denotes the gravitational acceleration vector. Equation 2.1 is the *continuity equation* and describes conservation of mass. Equation 2.2 is the *equation of motion* and describes conservation of momentum. Equation 2.3 is the *equation of energy conservation*. We can use equation 2.2 to neatly demonstrate how an outflow can be driven. I have deliberately written the equation so that all the force terms lie on the RHS. We can then see that for an outflow to be driven from an accreting object one simply needs one of the terms on the RHS to dominate over gravity, $\rho\vec{g}$. These terms thus signify three potential driving mechanisms.

- Magnetic Forces, $\frac{1}{4\pi}(\nabla \times \vec{B}) \times \vec{B}$.
- Radiative Forces, $\rho\vec{F}_{rad}$.
- Thermal Pressure, $-\nabla P$.

We can now examine under what physical conditions (and in which corresponding astrophysical objects) we might expect these forces to overcome gravity and cause a parcel of mass to escape to infinity. In other words: *what might drive a wind?*

2.2.1 Thermal Winds

In hydrostatic equilibrium (HSE), thermal pressure balances gravity and no other forces are present, meaning that the equation of motion can be written as

$$\rho \frac{Dv}{Dt} = -\nabla P + \rho\vec{g} = 0 \tag{2.4}$$

Clearly, if the thermal pressure is then significantly increased then this equilibrium condition no longer holds. This can occur in accretion discs at temperatures in excess of $\sim 10^7$ K – where other forces are negligible compared to thermal pressure – and where the escape velocities are relatively low (i.e. far out in the disc). Due to the temperature and gravity scalings, this means that XRBs are natural candidates for showing evidence of thermally driven winds. The outer disc can be heated to the Compton temperature by the central X-ray source, potentially driving relatively high mass-loss rate outflows (Begelman et al. 1983; Woods et al. 1996). This driving mechanism has been proposed as a natural explanation for the ever-present equatorial outflows in soft state XRBs (Ponti et al. 2012). However, they are much less likely candidates in CVs and AGN **Discuss scaling arguments with equations?**.

2.2.2 Radiatively Driven Winds

2.2.3 Line-driven Winds

2.2.4 Magneto-centrifugal Winds

2.3 Accretion Disc Wind Models

2.4 A Kinematic Prescription

2.5 The really, really big picture: AGN Feedback

The event horizon of a 10^9 $M_\odot$ BH is approximately 10^{15} cm, a billionth of the size of a typical galactic bulge. This is roughly the difference in size between a small coin and the radius of the Earth. Despite this vast different in scale, there are multiple pieces of evidence that the physics on the scale of the gravitational radius of the BH really does affect the evolution and dynamics of its host galaxy. I shall briefly discuss the evidence for this statement, and assess the potential role of winds together with alternative mechanisms.

2.5.1 Observational evidence for feedback

Perhaps the most famous pieces of evidence for some kind of long-distance relationship between a central BH and its host galaxy are the $M_{BH} - \sigma_*$ and $M_{BH} - M_{bulge}$ correlations, shown in figures **??** and 2.7 respectively.

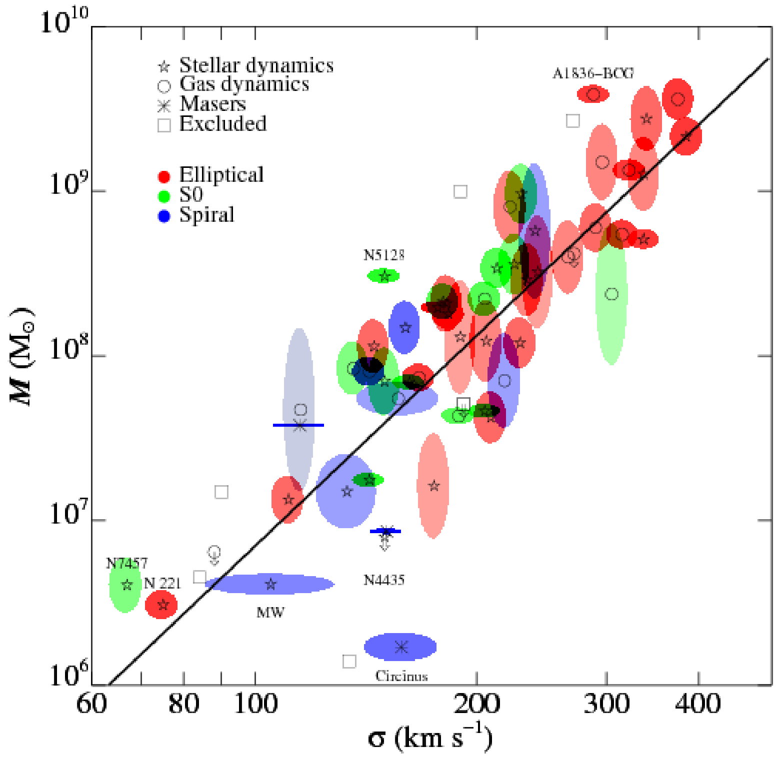

FIGURE 2.6: *Credit: Gultekin et al. 2009.* The $M_{BH} - \sigma_*$ correlation.

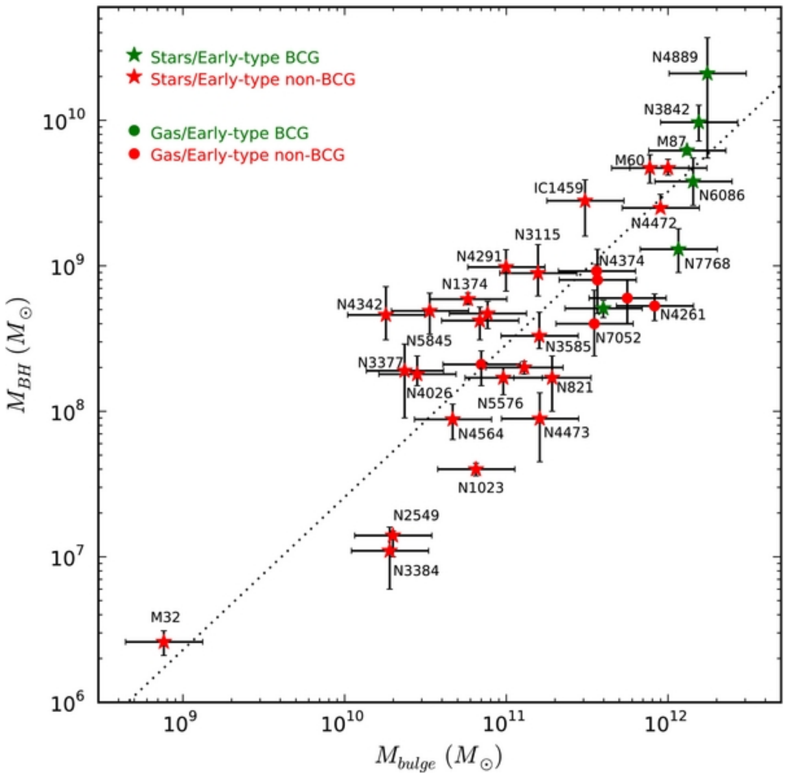

FIGURE 2.7: *Credit: McConell & Ma 2013.* The $M_{BH} - M_{bulge}$ correlation.

2.5.2 Radiative or quasar mode feedback

2.5.3 Kinetic or radio mode feedback

2.5.4 In-situ Explanations

Bibliography

Allen, J. T., P. C. Hewett, N. Maddox, G. T. Richards, and V. Belokurov
2011. A strong redshift dependence of the broad absorption line quasar fraction. *MNRAS*, 410:860–884.

Antonucci, R.
2013. Astrophysics: Quasars still defy explanation. *Nature*, 495:165–167.

Antonucci, R. R. J. and J. S. Miller
1985. Spectropolarimetry and the nature of NGC 1068. *ApJ*, 297:621–632.

Arévalo, P. and P. Uttley
2006. Investigating a fluctuating-accretion model for the spectral-timing properties of accreting black hole systems. *MNRAS*, 367:801–814.

Baldi, R. D., A. Capetti, A. Robinson, A. Laor, and E. Behar
2016. Radio-loud Narrow Line Seyfert 1 under a different perspective: a revised black hole mass estimate from optical spectropolarimetry. *MNRAS*.

Baptista, R., C. Silveira, J. E. Steiner, and K. Horne
2000. Spatially resolved spectra of the accretion disc of the nova-like variable UU Aquarii. *MNRAS*, 314:713–726.

Bartlett, E.
2013. *High mass X-ray binaries in the MilkyWay and beyond: a multiwavelength temporal and spectroscopic study*. PhD thesis, University of Southampton.

Begelman, M. C., C. F. McKee, and G. A. Shields
1983. Compton heated winds and coronae above accretion disks. I Dynamics. *ApJ*, 271:70–88.

Belloni, T., ed.
2010. *The Jet Paradigm*, volume 794 of *Lecture Notes in Physics, Berlin Springer Verlag.*

Benz, A. O., E. Fuerst, and A. L. Kiplinger
1983. First detection of radio emission from a dwarf nova. *Nature*, 302:45.

Bondi, H.
1952. On spherically symmetrical accretion. *MNRAS*, 112:195.

Bondi, H. and F. Hoyle
1944. On the mechanism of accretion by stars. *MNRAS*, 104:273.

Capellupo, D. M., H. Netzer, P. Lira, B. Trakhtenbrot, and J. Mejía-Restrepo
2015. Active galactic nuclei at z = 1.5 - I. Spectral energy distribution and accretion discs. *MNRAS*, 446:3427–3446.

Cassinelli, J. P.
1979. Stellar winds. *ARAA*, 17:275–308.

Cohen, R. D., R. C. Puetter, R. J. Rudy, T. B. Ake, and C. B. Foltz
1986. Variability of Markarian 1018 - Seyfert 1.9 to Seyfert 1. *ApJ*, 311:135–141.

Coppejans, D. L., E. G. Körding, J. C. A. Miller-Jones, M. P. Rupen, C. Knigge, G. R. Sivakoff, and P. J. Groot
2015. Novalike cataclysmic variables are significant radio emitters. *MNRAS*, 451:3801–3813.

Cordova, F. A. and K. O. Mason
1982. High-velocity winds from a dwarf nova during outburst. *ApJ*, 260:716–721.

Denney, K. D., G. De Rosa, K. Croxall, A. Gupta, M. C. Bentz, M. M. Fausnaugh, C. J. Grier, P. Martini, S. Mathur, B. M. Peterson, R. W. Pogge, and B. J. Shappee
2014. The Typecasting of Active Galactic Nuclei: Mrk 590 no Longer Fits the Role. *ApJ*, 796:134.

Dexter, J. and E. Agol
2011. Quasar Accretion Disks are Strongly Inhomogeneous. *ApJ Letters*, 727:L24.

Dhillon, V. S.

1996. The Nova-like variables. In *IAU Colloq. 158: Cataclysmic Variables and Related Objects*, A. Evans and J. H. Wood, eds., volume 208 of *Astrophysics and Space Science Library*, P. 3.

Dhillon, V. S. and R. G. M. Rutten

1995. Spectropolarimetry of the nova-like variable V 1315 Aquilae. *MNRAS*, 277:777–780.

Díaz Trigo, M. and L. Boirin

2015. Accretion disc atmospheres and winds in low-mass X-ray binaries. *ArXiv e-prints*.

Done, C., S. W. Davis, C. Jin, O. Blaes, and M. Ward

2012. Intrinsic disc emission and the soft X-ray excess in active galactic nuclei. *MNRAS*, 420:1848–1860.

Done, C. and C. Jin

2015. The Mass and Spin of The Extreme Narrow Line Seyfert 1 Galaxy 1H0707-495 and Its Implications for The Trigger for Relativistic Jets. *ArXiv e-prints*.

Drew, J. and F. Verbunt

1985. Investigation of a wind model for cataclysmic variable ultraviolet resonance line emission. *MNRAS*, 213:191–213.

Edelson, R., J. M. Gelbord, K. Horne, I. M. McHardy, B. M. Peterson, P. Arévalo, A. A. Breeveld, G. De Rosa, P. A. Evans, M. R. Goad, G. A. Kriss, W. N. Brandt, N. Gehrels, D. Grupe, J. A. Kennea, C. S. Kochanek, J. A. Nousek, I. Papadakis, M. Siegel, D. Starkey, P. Uttley, S. Vaughan, S. Young, A. J. Barth, M. C. Bentz, B. J. Brewer, D. M. Crenshaw, E. Dalla Bontà, A. De Lorenzo-Cáceres, K. D. Denney, M. Dietrich, J. Ely, M. M. Fausnaugh, C. J. Grier, P. B. Hall, J. Kaastra, B. C. Kelly, K. T. Korista, P. Lira, S. Mathur, H. Netzer, A. Pancoast, L. Pei, R. W. Pogge, J. S. Schimoia, T. Treu, M. Vestergaard, C. Villforth, H. Yan, and Y. Zu

2015. Space Telescope and Optical Reverberation Mapping Project. II. Swift and HST Reverberation Mapping of the Accretion Disk of NGC 5548. *ApJ*, 806:129.

Edge, D. O., J. R. Shakeshaft, W. B. McAdam, J. E. Baldwin, and S. Archer

1959. A survey of radio sources at a frequency of 159 Mc/s. *MmRA*, 68:37–60.

Eggleton, P. P.

1983. Approximations to the radii of Roche lobes. *ApJ*, 268:368.

Ehman, J. R., R. S. Dixon, and J. D. Kraus

1970. The Ohio survey between declinations of 0 and 36 south. *AJ*, 75:351–506.

Ekers, J. A.

1969. The Parkes catalogue of radio sources, declination zone +20 to -90 . *Australian Journal of Physics Astrophysical Supplement*, 7.

Elitzur, M.

2012. On the Unification of Active Galactic Nuclei. *ApJ Letters*, 747:L33.

Elitzur, M., L. C. Ho, and J. R. Trump

2014. Evolution of broad-line emission from active galactic nuclei. *MNRAS*, 438:3340–3351.

Elvis, M.

2000. A Structure for Quasars. *ApJ*, 545:63–76.

Elvis, M., B. J. Wilkes, J. C. McDowell, R. F. Green, J. Bechtold, S. P. Willner, M. S. Oey, E. Polomski, and R. Cutri

1994. Atlas of quasar energy distributions. *ApJs*, 95:1–68.

Fabian, A. C.

2012. Observational Evidence of Active Galactic Nuclei Feedback. *ARAA*, 50:455–489.

Fath, E. A.

1909. The spectra of some spiral nebulae and globular star clusters. *Lick Observatory Bulletin*, 5:71–77.

Fender, R. P.

2001. Powerful jets from black hole X-ray binaries in low/hard X-ray states. *MNRAS*, 322:31–42.

Fender, R. P., T. M. Belloni, and E. Gallo

2004. Towards a unified model for black hole X-ray binary jets. *MNRAS*, 355:1105–1118.

Frank, J., A. King, and D. Raine

1992. *Accretion power in astrophysics.*

Gierliński, M. and C. Done

2004. Is the soft excess in active galactic nuclei real? *MNRAS*, 349:L7–L11.

Gierliński, M. and C. Done

2006. Energy-dependent variability and the origin of the soft X-ray excess in active galactic nuclei. *MNRAS*, 371:L16–L20.

Greenstein, J. L. and J. B. Oke

1982. RW Sextantis, a disk with a hot, high-velocity wind. *ApJ*, 258:209–216.

Groot, P. J., R. G. M. Rutten, and J. van Paradijs

2004. A spectrophotometric study of RW Trianguli. *A&A*, 417:283–291.

Gültekin, K., D. O. Richstone, K. Gebhardt, T. R. Lauer, S. Tremaine, M. C. Aller, R. Bender, A. Dressler, S. M. Faber, A. V. Filippenko, R. Green, L. C. Ho, J. Kormendy, J. Magorrian, J. Pinkney, and C. Siopis

2009. The M-σ and M-L Relations in Galactic Bulges, and Determinations of Their Intrinsic Scatter. *ApJ*, 698:198–221.

Haardt, F. and L. Maraschi

1991. A two-phase model for the X-ray emission from Seyfert galaxies. *ApJ Letters*, 380:L51–L54.

Häring, N. and H.-W. Rix

2004. On the Black Hole Mass-Bulge Mass Relation. *ApJ Letters*, 604:L89–L92.

Hassall, B. J. M.

1985. A superoutburst of the dwarf nova EK Trianguli Australis. *MNRAS*, 216:335–352.

Haug, K.

1987. Continuum distributions and line profiles of UX UMA-type novalike systems. *AP&SS*, 130:91–102.

Hazard, C., M. B. Mackey, and A. J. Shimmins

1963. Investigation of the Radio Source 3C 273 By The Method of Lunar Occultations. *Nature*, 197:1037–1039.

Heap, S. R., A. Boggess, A. Holm, D. A. Klinglesmith, W. Sparks, D. West, C. C. Wu, A. Boksenberg, A. Willis, R. Wilson, F. Macchetto, P. O. Selvelli, D. Stickland, J. L. Greenstein, J. B. Hutchings, A. B. Underhill, R. Viotti, and J. A. J. Whelan
1978. IUE observations of hot stars - HZ43, BD +75 deg 325, NGC 6826, SS Cygni, Eta Carinae. *Nature*, 275:385–388.

Heil, L. M., S. Vaughan, and P. Uttley
2012. The ubiquity of the rms-flux relation in black hole X-ray binaries. *MNRAS*, 422:2620–2631.

Hessman, F. V., E. L. Robinson, R. E. Nather, and E.-H. Zhang
1984. Time-resolved spectroscopy of SS Cygni at minimum and maximum light. *ApJ*, 286:747–759.

Higginbottom, N., C. Knigge, K. S. Long, S. A. Sim, and J. H. Matthews
2013. A simple disc wind model for broad absorption line quasars. *MNRAS*, 436:1390–1407.

Hogg, J. D. and C. Reynolds
2015. Testing the Propagating Fluctuations Model with a Long, Global Accretion Disk Simulation. *ArXiv e-prints*.

Honeycutt, R. K., E. M. Schlegel, and R. H. Kaitchuck
1986. Evidence for a bipolar wind in the cataclysmic variable PG 1012-029. *ApJ*, 302:388–402.

Hönig, S. F., M. Kishimoto, K. R. W. Tristram, M. A. Prieto, P. Gandhi, D. Asmus, R. Antonucci, L. Burtscher, W. J. Duschl, and G. Weigelt
2013. Dust in the Polar Region as a Major Contributor to the Infrared Emission of Active Galactic Nuclei. *ApJ*, 771:87.

Horne, K.
1993. *Eclipse Mapping of Accretion Disks: The First Decade*, P. 117.

Horne, K. and T. R. Marsh
1986. Emission line formation in accretion discs. *MNRAS*, 218:761–773.

Hoyle, F. and R. A. Lyttleton
1939. The effect of interstellar matter on climatic variation. *Proceedings of the Cambridge Philosophical Society*, 35:405.

Idan, I., J.-P. Lasota, J.-M. Hameury, and G. Shaviv
2010. Accretion-disc model spectra for dwarf-nova stars. *A&A*, 519:A117.

Ioannou, Z., L. van Zyl, T. Naylor, P. A. Charles, B. Margon, L. Koch-Miramond, and S. Ilovaisky
2003. Understanding the LMXB X2127+119 in M 15. II. The UV data. *A&A*, 399:211–218.

Janiuk, A., B. Czerny, and G. M. Madejski
2001. The Nature of the Emission Components in the Quasar/NLS1 PG 1211+143. *ApJ*, 557:408–420.

Kafka, S. and R. K. Honeycutt
2004. Detecting Outflows from Cataclysmic Variables in the Optical. *AJ*, 128:2420–2429.

King, A.
2003. Black Holes, Galaxy Formation, and the M_{BH}-σ Relation. *ApJ Letters*, 596:L27–L29.

Knigge, C., I. Baraffe, and J. Patterson
2011. The Evolution of Cataclysmic Variables as Revealed by Their Donor Stars. *ApJs*, 194:28.

Knigge, C. and J. E. Drew
1997. Eclipse Mapping of the Accretion Disk Wind in the Cataclysmic Variable UX Ursae Majoris. *ApJ*, 486:445–456.

Knigge, C., K. S. Long, W. P. Blair, and R. A. Wade
1997. Disks, Winds, and Veiling Curtains: Dissecting the Ultraviolet Spectrum of the Dwarf Nova Z Camelopardalis in Outburst. *ApJ*, 476:291–310.

Knigge, C., K. S. Long, R. A. Wade, R. Baptista, K. Horne, I. Hubeny, and R. G. M. Rutten
1998a. Hubble Space Telescope Eclipse Observations of the Nova-like Cataclysmic Variable UX Ursae Majoris. *ApJ*, 499:414–428.

Knigge, C., K. S. Long, R. A. Wade, R. Baptista, K. Horne, I. Hubeny, and R. G. M. Rutten
1998b. Hubble Space Telescope Eclipse Observations of the Nova-like Cataclysmic Variable UX Ursae Majoris. *ApJ*, 499:414.

Knigge, C., S. Scaringi, M. R. Goad, and C. E. Cottis
2008. The intrinsic fraction of broad-absorption line quasars. *MNRAS*, 386:1426–1435.

Körding, E., M. Rupen, C. Knigge, R. Fender, V. Dhawan, M. Templeton, and T. Muxlow
2008. A Transient Radio Jet in an Erupting Dwarf Nova. *Science*, 320:1318–.

Kotov, O., E. Churazov, and M. Gilfanov
2001. On the X-ray time-lags in the black hole candidates. *MNRAS*, 327:799–807.

Kraft, R. P., J. Mathews, and J. L. Greenstein
1962. Binary Stars among Cataclysmic Variables. II. Nova WZ Sagittae: a Possible Radiator of Gravitational Waves. *ApJ*, 136:312–315.

Krolik, J. H. and M. C. Begelman
1986. The Dynamical State of the Obscuring Torus in Seyfert Galaxies. In *Bulletin of the American Astronomical Society*, volume 18 of *BAAS*, P. 903.

Kuulkers, E., S. Motta, J. Kajava, J. Homan, R. Fender, and P. Jonker
2015. Renewed activity of V404 Cyg (GS 2023+338). *The Astronomer's Telegram*, 7647.

La Dous, C.
1989. On the Balmer jump in dwarf novae during the outburst. *MNRAS*, 238:935–943.

Lasota, J.-P.
2001. The disc instability model of dwarf novae and low-mass X-ray binary transients. *NAR*, 45:449–508.

Liebert, J. and H. S. Stockman

1985. The AM Herculis magnetic variables. In *Cataclysmic Variables and Low-Mass X-ray Binaries*, D. Q. Lamb and J. Patterson, eds., volume 113 of *Astrophysics and Space Science Library*, Pp. 151–177.

Long, K. S., W. P. Blair, A. F. Davidsen, C. W. Bowers, W. V. D. Dixon, S. T. Durrance, P. D. Feldman, R. C. Henry, G. A. Kriss, J. W. Kruk, H. W. Moos, O. Vancura, H. C. Ferguson, and R. A. Kimble

1991. Spectroscopy of Z Camelopardalis in outburst with the Hopkins Ultraviolet Telescope. *ApJ Letters*, 381:L25–L29.

Long, K. S. and C. Knigge

2002. Modeling the Spectral Signatures of Accretion Disk Winds: A New Monte Carlo Approach. *ApJ*, 579:725–740.

Long, K. S., R. A. Wade, W. P. Blair, A. F. Davidsen, and I. Hubeny

1994. Observations of the bright novalike variable IX Velorum with the Hopkins Ultraviolet Telescope. *ApJ*, 426:704–715.

Lynden-Bell, D.

1969. Galactic Nuclei as Collapsed Old Quasars. *Nature*, 223:690–694.

Lyubarskii, Y. E.

1997. Flicker noise in accretion discs. *MNRAS*, 292:679.

Madau, P., G. Ghisellini, and A. C. Fabian

1994. The Unified Seyfert Scheme and the Origin of the Cosmic X-Ray Background. *MNRAS*, 270:L17.

Magdziarz, P., O. M. Blaes, A. A. Zdziarski, W. N. Johnson, and D. A. Smith

1998. A spectral decomposition of the variable optical, ultraviolet and X-ray continuum of NGC 5548. *MNRAS*, 301:179–192.

Mangham, S. W., C. Knigge, J. H. Matthews, K. S. Long, S. A. Sim, and N. Higginbottom

in prep. The reverberation signatures of rotating disk winds in AGN.

Marinucci, A., S. Bianchi, G. Matt, D. M. Alexander, M. Baloković, F. E. Bauer, W. N. Brandt, P. Gandhi, M. Guainazzi, F. A. Harrison, K. Iwasawa, M. Koss, K. K. Madsen,

F. Nicastro, S. Puccetti, C. Ricci, D. Stern, and D. J. Walton
2016. NuSTAR catches the unveiling nucleus of NGC 1068. *MNRAS*, 456:L94–L98.

Marscher, A. P.
2006. Relativistic Jets in Active Galactic Nuclei. In *Relativistic Jets: The Common Physics of AGN, Microquasars, and Gamma-Ray Bursts*, P. A. Hughes and J. N. Bregman, eds., volume 856 of *American Institute of Physics Conference Series*, Pp. 1–22.

Marsh, T. R. and K. Horne
1990. Emission-line mapping of the dwarf nova IP Pegasi in outburst and quiescence. *ApJ*, 349:593–607.

Matt, G., M. Guainazzi, and R. Maiolino
2003. Changing look: from Compton-thick to Compton-thin, or the rebirth of fossil active galactic nuclei. *MNRAS*, 342:422–426.

Mauche, C. W. and J. C. Raymond
1987. IUE observations of the dwarf nova HL Canis Majoris and the winds of cataclysmic variables. *ApJ*, 323:690–713.

McConnell, N. J. and C.-P. Ma
2013. Revisiting the Scaling Relations of Black Hole Masses and Host Galaxy Properties. *ApJ*, 764:184.

McHardy, I. M., E. Koerding, C. Knigge, P. Uttley, and R. P. Fender
2006. Active galactic nuclei as scaled-up Galactic black holes. *Nature*, 444:730–732.

Morgan, C. W., C. S. Kochanek, N. D. Morgan, and E. E. Falco
2010. The Quasar Accretion Disk Size-Black Hole Mass Relation. *ApJ*, 712:1129–1136.

Motta, S., A. Beardmore, S. Oates, N. P. M. K. A. Sanna, E. Kuulkers, J. Kajava, and C. Sanchez-Fernanedz
2015. X-ray and optical/UV variability from V404 Cyg (GS 2023+338) observed by Swift (part 1 of 2). *The Astronomer's Telegram*, 7665.

Murray, N. and J. Chiang
1996. Wind-dominated optical line emission from accretion disks around luminous cataclysmic variable stars. *Nature*, 382:789–791.

Murray, N. and J. Chiang
1997. Disk Winds and Disk Emission Lines. *ApJ*, 474:91–103.

Murray, N., J. Chiang, S. A. Grossman, and G. M. Voit
1995. Accretion Disk Winds from Active Galactic Nuclei. *ApJ*, 451:498.

Neugebauer, G., J. B. Oke, E. E. Becklin, and K. Matthews
1979. Absolute spectral energy distribution of quasi-stellar objects from 0.3 to 10 microns. *ApJ*, 230:79–94.

Noebauer, U. M., K. S. Long, S. A. Sim, and C. Knigge
2010. The Geometry and Ionization Structure of the Wind in the Eclipsing Nova-like Variables RW Tri and UX UMa. *ApJ*, 719:1932–1945.

Patterson, J.
1994. The DQ Herculis stars. *PASP*, 106:209–238.

Patterson, J., R. Patino, J. R. Thorstensen, D. Harvey, D. R. Skillman, and F. A. Ringwald
1996. Periods and Quasiperiods in the Cataclysmic Variable BZ Camelopardalis. *AJ*, 111:2422.

Perley, R. A., J. W. Dreher, and J. J. Cowan
1984. The jet and filaments in Cygnus A. *ApJ Letters*, 285:L35–L38.

Ponti, G., R. P. Fender, M. C. Begelman, R. J. H. Dunn, J. Neilsen, and M. Coriat
2012. Ubiquitous equatorial accretion disc winds in black hole soft states. *MNRAS*, 422:L11.

Potash, R. I. and J. F. C. Wardle
1980. 4C 32.69 - A quasar with a radio jet. *ApJ*, 239:42–49.

Pounds, K. A. and J. N. Reeves
2009. Quantifying the fast outflow in the luminous Seyfert galaxy PG1211+143. *MNRAS*, 397:249–257.

Puccetti, S., F. Fiore, G. Risaliti, M. Capalbi, M. Elvis, and F. Nicastro
2007. Rapid N_H changes in NGC 4151. *MNRAS*, 377:607–616.

Puebla, R. E., M. P. Diaz, D. J. Hillier, and I. Hubeny
2011. A Method for the Study of Accretion Disk Emission in Cataclysmic Variables. I. The Model. *ApJ*, 736:17.

Reeves, J. N., P. T. O'Brien, and M. J. Ward
2003. A Massive X-Ray Outflow from the Quasar PDS 456. *ApJ Letters*, 593:L65–L68.

Ringwald, F. A. and T. Naylor
1998. High-speed optical spectroscopy of a cataclysmic variable wind - BZ Camelopardalis. *AJ*, 115:286.

Ross, R. R. and A. C. Fabian
2005. A comprehensive range of X-ray ionized-reflection models. *MNRAS*, 358:211–216.

Rottenberg, J. A.
1952. Theoretical line profiles for stars of P Cygni type. *MNRAS*, 112:125.

Rutten, R. G. M., J. van Paradijs, and J. Tinbergen
1992. Reconstruction of the accretion disk in six cataclysmic variable stars. *A&A*, 260:213–226.

Scaringi, S., E. Körding, P. Uttley, C. Knigge, P. J. Groot, and M. Still
2012. The universal nature of accretion-induced variability: the rms-flux relation in an accreting white dwarf. *MNRAS*, 421:2854–2860.

Scaringi, S., T. J. Maccarone, E. Koerding, C. Knigge, S. Vaughan, T. R. Marsh, E. Aranzana, V. Dhillon, and S. C. C. Barros
2015. Accretion-induced variability links young stellar objects, white dwarfs, and black holes. *ArXiv e-prints*.

Seyfert, C. K.
1943. Nuclear Emission in Spiral Nebulae. *ApJ*, 97:28.

Shakura, N. I. and R. A. Sunyaev
1973. Black holes in binary systems. Observational appearance. *A&A*, 24:337–355.

Shaviv, G. and R. Wehrse
1991. Continuous energy distributions of accretion discs. *A&A*, 251:117–132.

Shi, Y., G. H. Rieke, P. Smith, J. Rigby, D. Hines, J. Donley, G. Schmidt, and A. M. Diamond-Stanic
2010. Unobscured Type 2 Active Galactic Nuclei. *ApJ*, 714:115–129.

Shlosman, I. and P. Vitello
1993. Winds from accretion disks - Ultraviolet line formation in cataclysmic variables. *ApJ*, 409:372–386.

Silk, J. and M. J. Rees
1998. Quasars and galaxy formation. *A&A*, 331:L1–L4.

Smak, J.
1981. On the Emission Lines from Rotating Gaseous Disks. *ACTAA*, 31:395.

Springel, V., T. Di Matteo, and L. Hernquist
2005. Black Holes in Galaxy Mergers: The Formation of Red Elliptical Galaxies. *ApJ Letters*, 620:L79–L82.

Struve, O.
1935. The Spectrum of P Cygni. *ApJ*, 81:66.

Tohline, J. E. and D. E. Osterbrock
1976. Variation of the spectrum of the Seyfert galaxy NGC 7603. *ApJ Letters*, 210:L117–L120.

Tombesi, F., M. Cappi, J. N. Reeves, G. G. C. Palumbo, T. Yaqoob, V. Braito, and M. Dadina
2010. Evidence for ultra-fast outflows in radio-quiet AGNs. I. Detection and statistical incidence of Fe K-shell absorption lines. *A&A*, 521:A57.

Tran, H. D.
2001. Hidden Broad-Line Seyfert 2 Galaxies in the CFA and 12 μM Samples. *ApJ Letters*, 554:L19–L23.

Urry, C. M. and P. Padovani
1995. Unified Schemes for Radio-Loud Active Galactic Nuclei. *PASP*, 107:803.

Uttley, P. and I. M. McHardy
2001. The flux-dependent amplitude of broadband noise variability in X-ray binaries and active galaxies. *MNRAS*, 323:L26–L30.

Uttley, P., I. M. McHardy, and S. Vaughan
2005. Non-linear X-ray variability in X-ray binaries and active galaxies. *MNRAS*, 359:345–362.

Van de Sande, M., S. Scaringi, and C. Knigge
2015. The rms-flux relation in accreting white dwarfs: another nova-like variable and the first dwarf nova. *MNRAS*, 448:2430–2437.

Wade, R. A.
1984. A double grid of accretion disc model spectra for cataclysmic variable stars. *MNRAS*, 208:381–398.

Wade, R. A.
1988. A test of synthetic accretion disk spectra using ultraviolet flux distributions of novalike variables. *ApJ*, 335:394–405.

Wang, B. and Z. Han
2012. Progenitors of type Ia supernovae. *NAR*, 56:122–141.

Warner, B.
2003. *Cataclysmic Variable Stars*.

Weymann, R. J., S. L. Morris, C. B. Foltz, and P. C. Hewett
1991. Comparisons of the emission-line and continuum properties of broad absorption line and normal quasi-stellar objects. *ApJ*, 373:23–53.

Woltjer, L.
1959. Emission Nuclei in Galaxies. *ApJ*, 130:38.

Woods, D. T., R. I. Klein, J. I. Castor, C. F. McKee, and J. B. Bell
1996. X-Ray–heated Coronae and Winds from Accretion Disks: Time-dependent Two-dimensional Hydrodynamics with Adaptive Mesh Refinement. *ApJ*, 461:767.

Zakamska, N. L., M. A. Strauss, J. H. Krolik, M. J. Collinge, P. B. Hall, L. Hao, T. M. Heckman, Ž. Ivezić, G. T. Richards, D. J. Schlegel, D. P. Schneider, I. Strateva, D. E. Vanden Berk, S. F. Anderson, and J. Brinkmann
2003. Candidate Type II Quasars from the Sloan Digital Sky Survey. I. Selection and Optical Properties of a Sample at 0.3¡Z¡0.83. *AJ*, 126:2125–2144.